Weakly nonlinear dynamics of a chemically active particle near the threshold for spontaneous motion. II. History-dependent motion

Gunnar G. Peng and Ory Schnitzer
Department of Mathematics, Imperial College London, London SW7 2AZ, United Kingdom

(Received 17 November 2022; accepted 22 February 2023; published 13 March 2023)

We develop a reduced model for the slow unsteady dynamics of an isotropic chemically active particle near the threshold for spontaneous motion. Building on the steady theory developed in part I of this series, we match a weakly nonlinear expansion valid on the particle scale with a leading-order approximation in a larger-scale unsteady remote region, where the particle acts as a moving point source of diffusing concentration. The resulting amplitude equation for the velocity of the particle includes a term representing the interaction of the particle with its own concentration wake in the remote region, which can be expressed as a time integral over the history of the particle motion, allowing efficient simulation and theoretical analysis of fully three-dimensional unsteady problems. To illustrate how to use the model, we study the effects of a weak force acting on the particle, including the stability of the steady states and how the velocity vector realigns toward the stable one, neither of which previous axisymmetric and steady models were able to capture. This unsteady formulation could also be applied to most of the other perturbation scenarios studied in part I as well as the dynamics of interacting active particles.

DOI: 10.1103/PhysRevFluids.8.033602

I. INTRODUCTION

This is the second part of a series of papers developing a weakly nonlinear theory for the dynamics of chemically active particles near the threshold for spontaneous motion. The starting point for the theory is the canonical model proposed by Michelin *et al.* [1] describing an autocatalytic colloid that self-propels despite having uniform surface properties, the underlying mechanism being a hydrochemical instability that can occur when diffusion is sufficiently weak relative to advection. While in practice diffusion dominates in experiments involving autocatalytic colloids [2,3], the canonical active-particle model serves as a simplified yet physically consistent reference model for self-solubilizing chemically active drops whose spontaneous motion has been observed in many experiments (see the recent review [4] and references therein). As discussed in the first part of this series [5] (henceforth "part I"), weakly nonlinear analyses of the canonical active-particle model and similar models of self-solubizing active drops have previously been limited to steady, axisymmetric solutions [6–10]. Building on those works, this series aims at an unsteady, three-dimensional theory that is also versatile in the sense that various perturbation effects can be easily included.

In part I, we revisited the weakly nonlinear analysis of the canonical model in the steady case. The key contribution of that part was the identification of the adjoint linearized differential operator and auxiliary conditions at the threshold. This allowed us to circumvent the apparent need in previous studies to directly solve the inhomogeneous linear problem at second order of the weakly nonlinear expansion. Rather, we used a Fredholm Alternative argument to extract a solvability condition on that inhomogeneous problem directly from its formulation, thereby obtaining the nonlinear amplitude equation governing the steady-state particle velocity. While

this contribution may seem merely technical, it in fact enables significant simplification and generalization. In particular, it effectively eliminates the difficulty in analyzing three-dimensional (in contrast to collinear/axisymmetric) particle motion and makes it straightforward to study the influence of weak perturbations from the canonical model, which generally have a leading-order effect on the particle velocity sufficiently near the threshold. We extensively demonstrated the efficacy of this approach by showing how the singular-pitchfork bifurcation previously established for isotropic active particles [8–11] is modified when various perturbations are included such as external force or torque fields, nonuniform surface perturbations and surface and bulk chemical kinetics.

In this part, we shall extend the steady weakly nonlinear theory developed in part I to the unsteady case. The motivation for such an extension is clear, namely to allow one to study the stability of steady states, transients and explore more complex unsteady phenomena that may arise when various perturbation effects are included into the modeling.

Following the steady case, our analysis will be based on asymptotic matching of a particle-scale weakly nonlinear expansion with a leading-order approximation in a remote region describing the concentration wake associated with the particle's activity and motion. We will see that the particle velocity evolves on such a long timescale that the particle-scale weakly nonlinear expansion remains quasisteady at the relevant orders. As as consequence, we will be able to directly employ the particle-scale analysis from part I, including the adjoint formulation associated with that region. In contrast, the remote region will be seen to be unsteady already at leading order, requiring us to generalize the analysis of that region and its matching with the particle-scale region.

As anticipated in part I, the above picture will lead us to an unconventional manifestation of unsteadiness in the nonlinear amplitude equation for the particle velocity, namely as an integral over the history of the particle motion representing the interaction of the particle with its own wake. This history dependence is linked to the spatial nonuniformity of the weakly nonlinear expansion, much like the other, more familiar, unconventional features of this problem, such as the singular-pitchfork bifurcation in the unperturbed isotropic active-particle case and the fact that the amplitude equation arises from solvability at second, rather than third, order of the weakly nonlinear expansion [8–11].

To focus on this essentially novel aspect of the theory, the only perturbation to the canonical active-particle model we shall consider in this part is that of a weak (possibly time-dependent) external force. There are two good reasons for considering this particular perturbation. First, the problem of an isotropic active particle or drop in an external force field has received considerable analytical [6,7,10,12], numerical [13], and experimental attention [14]. We note that weakly nonlinear analysis has been employed previously to calculate steady states in this scenario, in Ref. [10] and part I for the canonical active-particle model and before that in Refs. [6,7] for closely related active-drop models. Their stability, however, has so far only been guessed [10] or heuristically argued [6,7]. Second, it will be convenient to demonstrate stability predictions by considering the dynamics of particles disturbed from steady-state motion (force-free or forced) by localized-in-time force perturbations.

This paper continues as follows. In Sec. II, we formulate the canonical active-particle model with unsteadiness, and including a time-dependent external force. In Sec. III, we develop the unsteady weakly nonlinear theory building on the steady analysis of part I. The analysis in this section furnishes a preliminary form of the amplitude equation for the particle velocity, wherein unsteadiness enters via coupling with an initial-boundary-value problem in the remote region. In Sec. IV, we show by analysis of that problem that unsteadiness can instead be represented by a nonlocal history operator, namely a time integral over the history of the particle motion. In Sec. V, we present theoretical and numerical predictions of our model for both force-free and forced particles. We give concluding remarks in Sec. VI.

II. PROBLEM FORMULATION

A. Isotropic chemically active particle with an external force

We adopt the canonical model of an isotropic chemically active particle proposed by Michelin *et al.* [1], except that following several subsequent studies we include the possibility of an external force [10,12,13]. The formulation is thus similar to that in part I of this series, specifically in the scenario where an external force is included, with the key difference that in this part we allow for unsteadiness.

Consider a homogeneous spherical particle of radius a_* immersed in an unbounded liquid of viscosity η_*, with an asterisk subscript indicating a dimensional quantity. Solute molecules dissolved in the liquid are transported by diffusion, with diffusivity D_*, as well as advection, with the concentration approaching a constant value far from the particle. (Only perturbations from this value will be important.) The chemical activity of the particle is represented by a uniform and constant solute flux j_* at the particle surface (positive into the liquid). The fluid is driven at the surface of the particle via a diffusio-osmotic slip mechanism such that the fluid velocity relative to the surface is locally proportional to the concentration surface gradient; the coefficient of proportionality b_*, namely the slip coefficient, or surface mobility, is uniform and constant.

It is assumed that the inertia of the particle and fluid can be neglected. The flow field is therefore governed by the Stokes (zero-Reynolds-number) limit of the Navier–Stokes equations and the motion of the particle is such that the net (i.e., hydrodynamic plus external) force and torque on the particle both vanish. In this study, we shall only include an external force, denoted by $\mathbf{F}^e_*(t_*)$, which depends on time t_*.

In the case where there is no force, it is known that instability and spontaneous motion occur only if $j_* b_* > 0$ [1]. This is also a necessary condition for enhanced translation in the case where there is a weak external force [10,13]. Without loss of generality, we shall assume that both j_* and b_* are positive.

B. Dimensionless formulation

We adopt the same dimensionless conventions as in part I: lengths are normalized by a_*, concentrations by $c_* = a_* j_*/D_*$, velocities by $u_* = j_* b_*/D_*$, stresses and pressures by $\eta_* u_*/a_*$, forces by $\eta_* u_* a_*$ and torques by $\eta_* u_* a_*^2$. Time is normalized by a_*/u_*. As shown in Fig. 1, we denote the corresponding position vector measured from the center of the particle by $\mathbf{r} = r\hat{\mathbf{e}}_r$, with $r = |\mathbf{r}|$ and $\hat{\mathbf{e}}_r$ a radial unit vector; the deviation of the solute concentration from its value at infinity by c (henceforth called concentration); the fluid velocity field in a nonrotating frame of reference that moves with the particle's centroid by $\mathbf{u}$; the associated pressure field by p; the centroid velocity by $\mathbf{U}$; and particle angular velocity by $\boldsymbol{\Omega}$. We denote time by t', reserving the usual notation t for a slow-time coordinate to be introduced in the next section for the purpose of a weakly nonlinear analysis. The external force is denoted by $\mathbf{F}^e$.

The concentration c satisfies the unsteady advection–diffusion equation

$$\mathrm{Pe}\left(\frac{\partial c}{\partial t'} + \mathbf{u}\cdot\nabla c\right) = \nabla^2 c, \tag{2.1}$$

where

$$\mathrm{Pe} = \frac{a_* u_*}{D_*} \tag{2.2}$$

is an "intrinsic" Péclet number measuring the importance of advection relative to diffusion; the boundary condition

$$\frac{\partial c}{\partial r} = -1 \quad \text{at } r = 1 \tag{2.3}$$

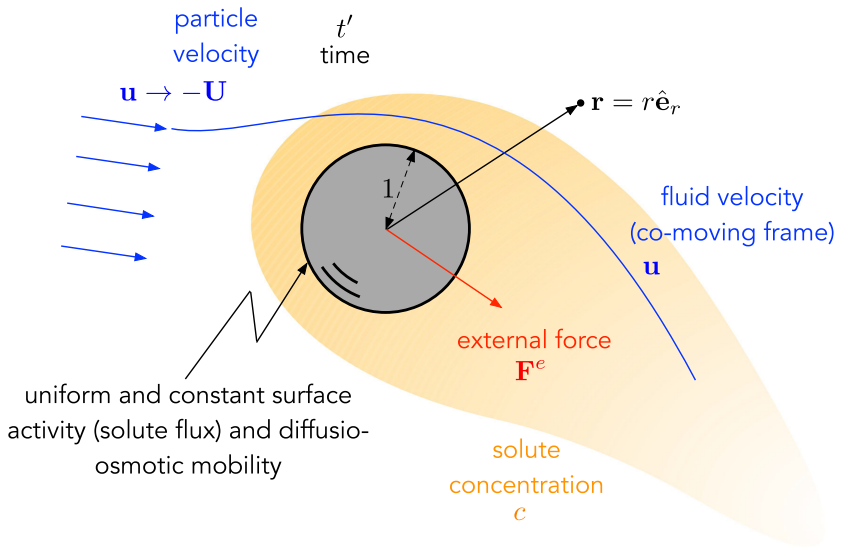

FIG. 1. Dimensionless schematic of a forced isotropic active particle. The angular velocity of the particle turns out to vanish trivially.

and decay condition

$$c \to 0 \quad \text{as} \quad r \to \infty. \tag{2.4}$$

The flow $\mathbf{u}$ and pressure p satisfy the Stokes equations

$$\boldsymbol{\nabla} \cdot \mathbf{u} = 0, \tag{2.5a}$$

$$\boldsymbol{\nabla} \cdot \boldsymbol{\sigma} = \mathbf{0}, \tag{2.5b}$$

in which

$$\boldsymbol{\sigma} = -p\mathsf{I} + \boldsymbol{\nabla}\mathbf{u} + (\boldsymbol{\nabla}\mathbf{u})^{\dagger} \tag{2.6}$$

is the stress tensor, I being the identity tensor and $\dagger$ denoting the tensor transpose; the boundary condition

$$\mathbf{u} = \boldsymbol{\nabla}_s c + \boldsymbol{\Omega} \times \mathbf{r} \quad \text{at} \quad r = 1, \tag{2.7}$$

in which $\boldsymbol{\nabla}_s = (\mathsf{I} - \hat{\mathbf{e}}_r\hat{\mathbf{e}}_r) \cdot \boldsymbol{\nabla}$ is the surface-gradient operator; the far-field condition

$$\mathbf{u} \to -\mathbf{U} \quad \text{as} \quad r \to \infty; \tag{2.8}$$

and the integral conditions

$$\mathbf{F} + \mathbf{F}^e = \mathbf{0}, \tag{2.9a}$$

$$\mathbf{T} = \mathbf{0}, \tag{2.9b}$$

where the hydrodynamic force $\mathbf{F}$ and torque $\mathbf{T}$ are defined by

$$\mathbf{F} = \oint_{r=1} dA\, \hat{\mathbf{e}}_r \cdot \boldsymbol{\sigma}, \tag{2.10a}$$

$$\mathbf{T} = \oint_{r=1} dA\, \mathbf{r} \times (\hat{\mathbf{e}}_r \cdot \boldsymbol{\sigma}), \tag{2.10b}$$

wherein dA is an infinitesimal area element. As the Stokes equations (2.5) are homogeneous, the pressure p should be interpreted as a modified pressure with any deviation from neutral buoyancy of the particle included in the external force.

In principle, it is necessary to also prescribe initial conditions to close the problem formulation. Since the flow problem is instantaneous, it suffices to prescribe the concentration field at some given moment. We shall return to this point in the next section.

For the problem formulated above, it can be shown that the angular velocity $\mathbf{\Omega}$ vanishes trivially. This follows from an application of the reciprocal theorem to spherical phoretic particles as in Ref. [15], noting the absence of an external torque [cf. Eq. (2.9b)] and the fact that the relative surface velocity is given by the surface gradient of a smooth scalar field [cf. Eq. (2.7)]. We shall not rely on this exact result so that the analysis in the next section appears as close as possible to that in part I. This will help to simplify future extensions of the unsteady analysis in this part to include perturbation effects that give rise to particle rotation.

III. UNSTEADY WEAKLY NONLINEAR THEORY

A. Weakly nonlinear regime and slow timescale

In the absence of an external force, there exists a steady solution for all values of the Péclet number such that the particle and fluid are stationary and the concentration is spherically distributed, $c = c_0(r)$, with

$$c_0 = \frac{1}{r}. \tag{3.1}$$

The linear stability analysis in Ref. [1], which assumes axisymmetric perturbations, shows that this stationary–symmetric base state is unstable for $\mathrm{Pe} > 4$, with a positive growth rate (normalized by u_*/a_*) scaling like $(\mathrm{Pe} - 4)^2$ as $\mathrm{Pe} \searrow 4$. This scaling suggests that near the instability threshold the dynamics of the particle evolve on long times scaling like $1/(\mathrm{Pe} - 4)^2$, the physical significance of which will become evident later. It is further known, based on the steady analyses in part I and Ref. [10], that even a weak external force can have a leading-order effect on the motion of the particle sufficiently near the threshold, specifically for $\mathrm{Pe} - 4 = \mathcal{O}(|\mathbf{F}^e|^{1/2})$.

Our goal here is to describe the unsteady dynamics of the particle near the instability threshold, including the effect of a weak external force. As in part I, we write

$$\mathrm{Pe} = 4 + \epsilon\chi \tag{3.2}$$

and carry out a weakly nonlinear analysis as $\epsilon \searrow 0$, with χ a rescaled bifurcation parameter. In light of the above scalings, the concentration and flow fields are assumed to be functions of position $\mathbf{r}$ and the slow time coordinate

$$t = \epsilon^2 t', \tag{3.3}$$

such that, in particular, the advection–diffusion equation (2.1) is rewritten as

$$\mathrm{Pe}\left(\epsilon^2 \frac{\partial c}{\partial t} + \mathbf{u} \cdot \nabla c\right) = \nabla^2 c. \tag{3.4}$$

Furthermore, the external force is prescribed as

$$\mathbf{F}^e(t') = 6\pi\epsilon^2 \mathbf{f}(t), \tag{3.5}$$

so that it varies on the characteristic timescale and is just strong enough to have a leading-order effect on the particle motion.

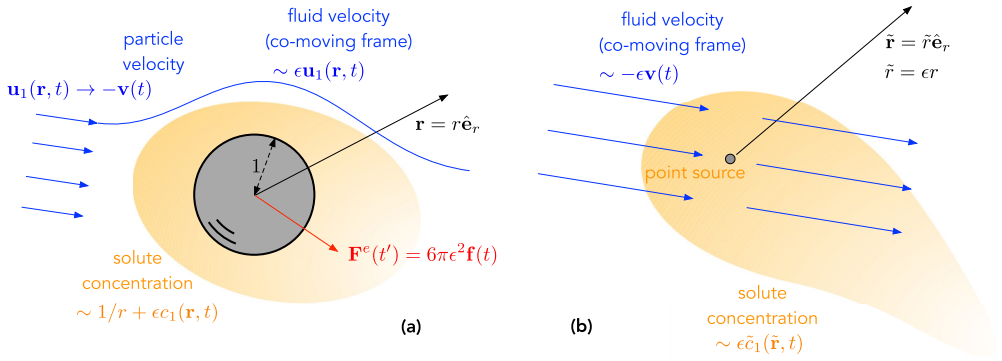

FIG. 2. Particle-scale (a) and remote (b) regions of the weakly nonlinear analysis near the instability threshold (Sec. III). The small positive parameter ϵ characterizes the shift of the Péclet number from its critical value [cf. Eq. (3.2)]. Note that $t = \epsilon^2 t'$ denotes a slow-time coordinate [cf. Eq. (3.3)].

B. Particle-scale weakly nonlinear expansions

We expand the concentration in powers of ϵ as

$$c(\mathbf{r},t;\epsilon) \sim c_0(r) + \epsilon c_1(\mathbf{r},t) + \epsilon^2 c_2(\mathbf{r},t) \quad \text{as} \quad \epsilon \searrow 0, \tag{3.6}$$

wherein c_0 is the equilibrium solution (3.1), and the flow as

$$\mathbf{u}(\mathbf{r},t;\epsilon) \sim \epsilon\mathbf{u}_1(\mathbf{r},t) + \epsilon^2\mathbf{u}_2(\mathbf{r},t), \tag{3.7a}$$

$$p(\mathbf{r},t;\epsilon) \sim \epsilon p_1(\mathbf{r},t) + \epsilon^2 p_2(\mathbf{r},t) \quad \text{as} \quad \epsilon \searrow 0. \tag{3.7b}$$

Quantities associated with the flow, including the hydrodynamic force $\mathbf{F}$, hydrodynamic torque $\mathbf{T}$, stress tensor $\boldsymbol{\sigma}$, and particle velocities $\mathbf{U}$ and $\boldsymbol{\Omega}$, are expanded similar to Eq. (3.7). For the particle velocity $\mathbf{U}$, we introduce the special notation $\mathbf{U}_1(t) = \mathbf{v}(t)$, such that

$$\mathbf{U}(t;\epsilon) \sim \epsilon\mathbf{v}(t) \quad \text{as} \quad \epsilon \searrow 0, \tag{3.8}$$

with $\mathbf{v}(t)$ corresponding to a rescaled leading-order approximation for the particle velocity. Given prior comments, we expect the expansion for $\boldsymbol{\Omega}$ to be trivial at all orders.

For the same reasons as discussed in part I, the concentration "particle-scale" expansion (3.6) breaks down at large distances $r = \mathrm{ord}(1/\epsilon)$ corresponding to a "remote region" where diffusion and advection are comparable and in particular $c_0 = 1/r$ does not hold as a leading-order approximation (see Fig. 2).

In the particle region, c_0 is independent of t and so the time derivative in Eq. (3.4) does not enter up to and including the order-ϵ^2 balance of that equation. Based on the steady analysis in part I, we do not expect higher-order terms to influence the leading-order dynamics of the particle. Thus, the particle-scale region is effectively quasistatic and hence its analysis follows closely the steady analysis in part I. In particular, we will be able to directly employ the solvability result derived in part I to circumvent the need to solve the particle-scale problem at order ϵ^2. The only difference arises from the far-field conditions satisfied by $c_1(\mathbf{r},t)$ and $c_2(\mathbf{r},t)$ as $r \to \infty$, which now need to be derived by matching with a generally unsteady, rather than steady, remote-region approximation.

We proceed with an analysis of the unsteady remote region (Sec. III C), after which it will be straightforward to utilize results from part I pertaining to the particle-scale expansions (3.6) and (3.7) to derive an unsteady nonlinear amplitude equation for $\mathbf{v}(t)$ (Sec. III D).

C. Unsteady remote region

Toward analyzing the remote region, we define $c(\mathbf{r}, t; \epsilon) = \tilde{c}(\tilde{\mathbf{r}}, t; \epsilon)$, where $\tilde{\mathbf{r}} = \epsilon \mathbf{r}$ is a strained position vector of magnitude $\tilde{r} = \epsilon r$. As in the steady analysis of part I, the $1/r$ decay of the leading-order particle-scale concentration [cf. Eq. (3.1)] implies the remote-region expansion

$$\tilde{c}(\tilde{\mathbf{r}}, t; \epsilon) \sim \epsilon \tilde{c}_1(\tilde{\mathbf{r}}, t) \quad \text{as} \quad \epsilon \searrow 0. \tag{3.9}$$

In contrast to the particle-scale concentration expansion (3.6), the flow expansions (3.7) are uniform in r. Accordingly, the far-field condition (2.8) together with the leading-order approximation (3.8) for the particle velocity together imply $\mathbf{u}(\tilde{\mathbf{r}}/\epsilon, t; \epsilon) \sim -\epsilon \mathbf{v}(t)$ as $\epsilon \searrow 0$. Thus, together with the Péclet-number rescaling (3.2), the advection–diffusion equation (3.4) gives

$$\frac{\partial \tilde{c}_1}{\partial t} - \mathbf{v} \cdot \tilde{\boldsymbol{\nabla}} \tilde{c}_1 = \frac{1}{4} \tilde{\nabla}^2 \tilde{c}_1, \tag{3.10}$$

for $\tilde{r} > 0$, in which $\tilde{\boldsymbol{\nabla}}$ is the gradient operator with respect to $\tilde{\mathbf{r}}$. The advection–diffusion equation (3.10), in which the advecting flow is a time-dependent uniform stream, is supplemented by the decay condition

$$\tilde{c}_1 \to 0 \quad \text{as} \quad \tilde{r} \to \infty, \tag{3.11}$$

which follows from Eq. (2.4), and the singular behavior

$$\tilde{c}_1 \sim \frac{1}{\tilde{r}} \quad \text{as} \quad \tilde{r} \searrow 0, \tag{3.12}$$

which follows from asymptotically matching the one-term remote-region expansion (3.9) and the particle-region concentration expansion (3.6) taken to leading order.

The problem (3.10)–(3.12) governing $\tilde{c}_1(\mathbf{r}, t)$ is schematically depicted in Fig. 2(b). It is an unsteady generalization of the steady remote-region problem encountered in part I. For the purpose of deriving far-field conditions on the particle-scale concentrations $c_1(\mathbf{r}, t)$ and $c_2(\mathbf{r}, t)$, what is important is the behavior of $\tilde{c}(\tilde{\mathbf{r}}, t)$ as $\tilde{\mathbf{r}} \searrow 0$. In Appendix A, we show by means of a local analysis of Eq. (3.10) as $\tilde{r} \searrow 0$, starting with Eq. (3.12), that the solution possesses an expansion of the form

$$\tilde{c}_1(\tilde{\mathbf{r}}, t) = \frac{1}{\tilde{r}} + \tilde{h}(t) - 2\mathbf{v}(t) \cdot \hat{\mathbf{e}}_r + \tilde{r}\{2\mathbf{v}(t)\mathbf{v}(t) : (\mathsf{I} + \hat{\mathbf{e}}_r \hat{\mathbf{e}}_r) + \hat{\mathbf{e}}_r \cdot \tilde{\mathbf{H}}(t)\} + o(\tilde{r}) \quad \text{as} \quad \tilde{r} \searrow 0, \tag{3.13}$$

in which $\tilde{h}(t)$ and $\tilde{\mathbf{H}}(t)$ are a scalar and a vector, respectively, that are left undetermined by the local analysis. Given a global, i.e., exact solution to the remote-region problem (3.10)–(3.12), these functions could be extracted at any time t by inspecting the behavior of the solution as $\tilde{r} \searrow 0$. We shall see that $\tilde{\mathbf{H}}(t)$ plays a role in determining the leading-order dynamics of the particle, whereas $\tilde{h}(t)$ does not.

In particular, for a steady particle velocity $\mathbf{v}(t) = \bar{\mathbf{v}}$ having magnitude $\bar{v}$, the remote-region problem (3.10)–(3.12) is known to possess the steady solution [16]

$$\tilde{c}_1^s(\tilde{\mathbf{r}}; \bar{\mathbf{v}}) = \frac{1}{\tilde{r}} \exp\{-2\bar{\mathbf{v}} \cdot \tilde{\mathbf{r}} - 2\bar{v}\tilde{r}\}, \tag{3.14}$$

which was also used in steady weakly nonlinear analyses of active particles [8–10]. It has the local expansion

$$\tilde{c}_1^s(\tilde{\mathbf{r}}; \bar{\mathbf{v}}) = \frac{1}{\tilde{r}} - 2\bar{v} - 2\bar{\mathbf{v}} \cdot \hat{\mathbf{e}}_r + \tilde{r}\{2\bar{\mathbf{v}}\bar{\mathbf{v}} : (\mathsf{I} + \hat{\mathbf{e}}_r \hat{\mathbf{e}}_r) + 4\bar{v}\bar{\mathbf{v}} \cdot \hat{\mathbf{e}}_r\} + o(r) \quad \text{as} \quad \tilde{r} \searrow 0. \tag{3.15}$$

Comparison of Eq. (3.15) with the general local expansion (3.13) gives, for $\mathbf{v}(t) \equiv \bar{\mathbf{v}}$,

$$\tilde{h}(t) \equiv -2\bar{v}, \tag{3.16a}$$

$$\tilde{\mathbf{H}}(t) \equiv 4\bar{v}\bar{\mathbf{v}}. \tag{3.16b}$$

One approach to obtain $\tilde{\mathbf{H}}(t)$ in the more general unsteady case is to solve the remote-region problem (3.10)–(3.12) numerically in three spatial dimensions plus time, starting from an initial distribution $\tilde{c}_1(\tilde{\mathbf{r}}, 0)$ that is compatible with Eqs. (3.11) and (3.12). In this approach, $\tilde{\mathbf{H}}(t)$ is in practice determined from the instantaneous remote-region distribution $\tilde{c}_1(\tilde{\mathbf{r}}, t)$. Given the form of the remote-region problem, it can also be conceptually considered as a time-dependent functional of the initial distribution $\tilde{c}_1(\tilde{\mathbf{r}}, 0)$ and the particle velocity $\mathbf{v}(\tau)$ over the interval $0 \leqslant \tau \leqslant t$.

In Sec. IV, we shall develop an alternative approach by analytically solving the unsteady remote-region problem. This will lead us to an explicit representation for $\tilde{\mathbf{H}}(t)$ in terms of a "history operator," namely an integral over the history of the particle motion without explicit reference to any concentration distribution. We shall adopt this approach in Sec. V toward studying the dynamics of force-free and forced active particles.

D. Unsteady amplitude equation

We proceed to consider the particle-scale region, closely following the steady theory in part I. We begin by noting that asymptotic matching between the particle-scale concentration expansion (3.6) taken up to order ϵ^2 and the leading-order remote-region concentration approximation (3.9), using the local behavior (3.13), yields the following far-field conditions on the particle-scale concentration fields:

$$c_1(\mathbf{r}, t) = \tilde{h}(t) - 2\hat{\mathbf{e}}_r \cdot \mathbf{v}(t) + o(1) \quad \text{as} \quad r \to \infty, \tag{3.17}$$

$$c_2(\mathbf{r}, t) = r\{2\mathbf{v}(t)\mathbf{v}(t) : (\mathsf{I} + \hat{\mathbf{e}}_r\hat{\mathbf{e}}_r) + \hat{\mathbf{e}}_r \cdot \tilde{\mathbf{H}}(t)\} + o(r) \quad \text{as} \quad r \to \infty. \tag{3.18}$$

With Eq. (3.17), we find from the governing equations (2.3)–(2.9) and (3.4) a homogeneous problem for the order-ϵ fields and particle velocities that is identical to that found in Sec. II E of part I, except that the spatially constant term in Eq. (3.17) is $\tilde{h}(t)$ instead of its steady-state value (3.16a). We thus have the general solution [cf. Eqs. (2.27)–(2.29), part I]

$$c_1(\mathbf{r}, t) = \tilde{h}(t) - \mathbf{v}(t) \cdot \left(\frac{2}{r} - \frac{3}{2r^3} + \frac{1}{r^4}\right)\mathbf{r}, \tag{3.19a}$$

$$\mathbf{u}_1(\mathbf{r}, t) = -\mathbf{v}(t) \cdot \left(\mathsf{I} - \frac{1}{2}\nabla\nabla\frac{1}{r}\right), \tag{3.19b}$$

$$p_1(\mathbf{r}, t) = 0, \tag{3.19c}$$

with the particle velocity $\mathbf{v}(t)$ undetermined at this stage (and the corresponding angular velocity $\boldsymbol{\Omega}_1(t) = \mathbf{0}$, as it must be given our previous comment that $\boldsymbol{\Omega}(t)$ is identically zero). The existence of nontrivial solutions to the homogeneous order-ϵ problem is a consequence of perturbing about the threshold for instability of a force-free particle; indeed, up to the nonlinear spatially constant term $\tilde{h}(t)$, the solutions (3.19) can be identified as the marginally stable modes of the full problem when linearized at the threshold $\mathrm{Pe} = 4$ [1].

With Eq. (3.18), we find from the governing equations (2.3)–(2.9) and (3.4) an inhomogeneous problem for the order-ϵ^2 fields and particle velocities. It is the same as that found in Sec. IV A of part I (see also Sec. II G therein for the case of a forced particle), except for the unsteady generalization of $\tilde{\mathbf{H}}(t)$ in Eq. (3.18) from its value (3.16b) for a constant particle velocity and of the force condition at this order to allow for a time-dependent force:

$$\mathbf{F}_2(t) = -6\pi\mathbf{f}(t). \tag{3.20}$$

The order-ϵ^2 problem is an inhomogeneous version of the homogeneous order-ϵ problem. As the latter possesses the nontrivial solutions (3.19), the former can only be solvable under certain conditions on the forcing terms. In part I, one of us developed an explicit solvability condition for a

generalized inhomogeneous problem that in the present case reduces to [cf. part I, Eq. (3.31)]

$$3\lim_{\lambda\to\infty}\frac{1}{\lambda^2}\oint_{r=\lambda} dA\,\hat{\mathbf{e}}_r\mathcal{R} - 2\pi\mathbf{f} = \lim_{\lambda\to\infty}\oint_{1<r<\lambda} dV\,\hat{\mathbf{e}}_r\frac{\mathcal{C}}{r^2}, \tag{3.21}$$

in which

$$\mathcal{C} = 4\mathbf{u}_1\cdot\boldsymbol{\nabla}c_1 + \chi\mathbf{u}_1\cdot\boldsymbol{\nabla}\frac{1}{r}, \tag{3.22a}$$

$$\mathcal{R} = 2\mathbf{v}\mathbf{v}:(\mathsf{I}+\hat{\mathbf{e}}_r\hat{\mathbf{e}}_r) + \hat{\mathbf{e}}_r\cdot\tilde{\mathbf{H}}. \tag{3.22b}$$

The field $\mathcal{C}$ differs from that in the steady analysis of an isotropic active particle [cf. part I, Eq. (3.32a)] only in that $\boldsymbol{\nabla}c_1$ and $\mathbf{u}_1$ are here proportional to the time-dependent particle velocity $\mathbf{v}(t)$ rather than necessarily a steady one [cf. Eq. (3.19)]. The field $\mathcal{R}$ differs from that in the above steady analysis [cf. part I, Eq. (3.32b)] in the unsteady generalization of $\tilde{\mathbf{H}}(t)$ from its value (3.16b) for a constant particle velocity. We therefore find, by either direct calculation or adapting results from part I,

$$\lim_{\lambda\to\infty}\oint_{1<r<\lambda} dV\,\hat{\mathbf{e}}_r\frac{\mathcal{C}}{r^2} = \chi\pi\mathbf{v}, \tag{3.23a}$$

$$\lim_{\lambda\to\infty}\frac{1}{\lambda^2}\oint_{r=\lambda} dA\,\hat{\mathbf{e}}_r\mathcal{R} = \frac{4\pi}{3}\tilde{\mathbf{H}}. \tag{3.23b}$$

The solvability condition (3.21) thus yields the requisite amplitude equation

$$\chi\mathbf{v} - 4\tilde{\mathbf{H}} + 2\mathbf{f} = 0. \tag{3.24}$$

In its present form, the amplitude equation (3.24) involves the vector quantity $\tilde{\mathbf{H}}(t)$. Its solution therefore entails the simultaneous solution of the remote-region problem formulated in Sec. III C—a linear initial-boundary-value problem in three spatial dimensions plus time. While this could be done numerically, we shall prefer to employ the analytical history-operator representation of $\tilde{\mathbf{H}}(t)$ to be developed in Sec. IV along with some of its properties. Readers not interested in this derivation may choose to skip directly to Sec. V, where we first recapitulate the amplitude equation formulated using the integral representation for $\tilde{\mathbf{H}}(t)$ and then study the dynamics of force-free and forced active particles based on that formulation.

IV. HISTORY OPERATOR

A. Solution of the unsteady remote problem

The vector quantity $\tilde{\mathbf{H}}(t)$ appearing in the amplitude equation (3.24) was defined in Sec. III C based on the local expansion (3.13) of the remote-region concentration field. In this section we shall develop an explicit representation for $\tilde{\mathbf{H}}(t)$ as an integral over the history of the particle motion. This representation is based on a general analytical solution to the unsteady remote-region problem (3.10)–(3.12), which we derive below.

It is convenient to reformulate the remote-region problem as follows. First, we combine the advection–diffusion equation (3.10) for $\tilde{r} > 0$ and the singular behavior (3.12) to find

$$\frac{\partial\tilde{c}_1}{\partial t} - \mathbf{v}\cdot\tilde{\boldsymbol{\nabla}}\tilde{c}_1 - \frac{1}{4}\tilde{\nabla}^2\tilde{c}_1 = \pi\delta(\tilde{\mathbf{r}}), \tag{4.1}$$

where $\delta(\tilde{\mathbf{r}})$ denotes the three-dimensional Dirac δ function such that the equation holds everywhere in the sense of distributions. Second, we move from the comoving frame to the laboratory frame by writing $c_1(\tilde{\mathbf{r}},t) = C(\boldsymbol{\rho},t)$, where $\boldsymbol{\rho} = \mathbf{x}(t) + \tilde{\mathbf{r}}$ is a (strained) position measured from a point fixed in the laboratory frame, with $\mathbf{x}(t)$ the corresponding particle location such that

$$\mathbf{v}(t) = \frac{d\mathbf{x}}{dt}, \tag{4.2}$$

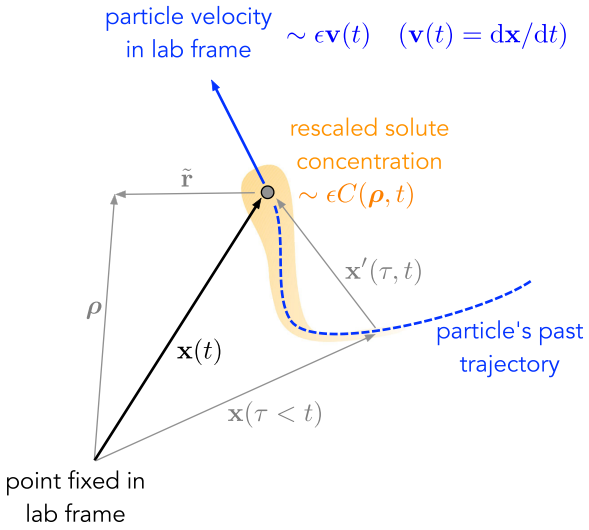

FIG. 3. In the laboratory frame, the remote-region problem consists of unsteady diffusion from a moving point source corresponding to the active particle.

as shown in Fig. 3. The advection–diffusion equation (4.1) is thus transformed into

$$\frac{\partial C}{\partial t} = \frac{1}{4}\nabla_{\boldsymbol{\rho}}^2 C + \pi\delta(\boldsymbol{\rho} - \mathbf{x}(t)), \tag{4.3}$$

wherein $\nabla_{\boldsymbol{\rho}}$ is the gradient operator with respect to $\boldsymbol{\rho}$. The laboratory-frame problem therefore consists of Eq. (4.3) and the decay condition

$$C(\boldsymbol{\rho}, t) \to 0 \quad \text{as} \quad |\boldsymbol{\rho}| \to \infty, \tag{4.4}$$

which follows from Eq. (3.11). This problem describes unsteady diffusion from a moving point source corresponding to the active particle.

To solve the laboratory-frame problem we introduce the Green's function $G(\boldsymbol{\rho}, t)$ satisfying

$$\frac{\partial G}{\partial t} - \frac{1}{4}\nabla_{\boldsymbol{\rho}}^2 G = \delta(t)\delta(\boldsymbol{\rho}), \tag{4.5}$$

wherein $\delta(t)$ denotes the one-dimensional Dirac δ function, together with $G(\boldsymbol{\rho}, t) = 0$ for $t < 0$ and $G(\boldsymbol{\rho}, t) \to 0$ as $\rho = |\boldsymbol{\rho}| \to \infty$. The solution is readily found using the Fourier transform and is well known to be (for $t > 0$)

$$G(\boldsymbol{\rho}, t) = \frac{1}{\pi^{3/2} t^{3/2}} e^{-\rho^2/t}. \tag{4.6}$$

By superposition we have

$$C(\boldsymbol{\rho}, t) = \pi \int_{-\infty}^{t} d\tau\, G[\boldsymbol{\rho} - \mathbf{x}(\tau), t - \tau]. \tag{4.7}$$

Going back to the original remote-region formulation,

$$\tilde{c}_1(\tilde{\mathbf{r}}, t) = \frac{1}{\sqrt{\pi}} \int_{-\infty}^{t} d\tau\, \frac{1}{(t-\tau)^{3/2}} \exp\left\{-\frac{|\mathbf{x}'(\tau, t) + \tilde{\mathbf{r}}|^2}{t - \tau}\right\}, \tag{4.8}$$

where we define the displacement

$$\mathbf{x}'(\tau, t) = \mathbf{x}(t) - \mathbf{x}(\tau) = \int_{\tau}^{t} \mathrm{d}s\, \mathbf{v}(s), \tag{4.9}$$

namely the position at time t measured from the position at the past time τ (see Fig. 3).

B. History operator

We can now extract $\tilde{\mathbf{H}}(t)$ by comparing the local expansion (3.13) with an asymptotic expansion of Eq. (4.8) as $\tilde{r} \searrow 0$. (This procedure will also provide $\tilde{h}(t)$ which does not enter the amplitude equation (3.24), but the result may be useful when including some perturbation effects as well as in other problems involving unsteady convective transport; see, e.g., Refs. [17,18].) The expansion for Eq. (4.8) is derived with the help of the subtraction

$$\tilde{c}_1(\tilde{\mathbf{r}}, t) = \tilde{c}_1^s[\tilde{\mathbf{r}}; \mathbf{v}(t)] + \Delta\tilde{c}_1(\tilde{\mathbf{r}}, t), \tag{4.10}$$

where the "quasisteady" contribution $\tilde{c}_1^s[\tilde{\mathbf{r}}; \mathbf{v}(t)]$ corresponds to the concentration field generated as if the particle has always been moving at its instantaneous velocity $\mathbf{v}(t)$ [cf. Eq. (3.14)], while $\Delta\tilde{c}_1(\tilde{\mathbf{r}}, t)$ is the concentration field owing to the deviation of the particle motion from that steady state. The singular small-$\tilde{r}$ behavior of the quasisteady contribution $\tilde{c}_1^s[\tilde{\mathbf{r}}; \mathbf{v}(t)]$ is provided by Eq. (3.15), with $\mathbf{v}(t)$ replacing $\bar{\mathbf{v}}$,

$$\tilde{c}_1^s[\tilde{\mathbf{r}}; \mathbf{v}(t)] = \frac{1}{\tilde{r}} - 2v(t) - 2\mathbf{v}(t)\cdot\hat{\mathbf{e}}_r + \tilde{r}\{2\mathbf{v}(t)\mathbf{v}(t) : (\mathsf{I} + \hat{\mathbf{e}}_r\hat{\mathbf{e}}_r) + 4v(t)\mathbf{v}(t)\cdot\hat{\mathbf{e}}_r\} + o(r) \quad \text{as} \quad \tilde{r} \searrow 0. \tag{4.11}$$

It therefore remains to consider the small-$\tilde{r}$ behavior of $\Delta\tilde{c}_1(\tilde{\mathbf{r}}, t)$. To this end, we begin by noting that an integral representation of the quasisteady contribution can be derived by substituting $\mathbf{x}(t) - \mathbf{x}(\tau) = (t-\tau)\mathbf{v}(t)$ into the general solution (4.8). This gives

$$\tilde{c}_1^s[\tilde{\mathbf{r}}; \mathbf{v}(t)] = \frac{1}{\sqrt{\pi}} \int_{-\infty}^{t} \frac{d\tau}{(t-\tau)^{3/2}} \exp\left\{-\frac{|(t-\tau)\mathbf{v}(t) + \tilde{\mathbf{r}}|^2}{t-\tau}\right\}. \tag{4.12}$$

We then find from Eq. (4.8) and the definition (4.10) that

$$\Delta\tilde{c}_1(\tilde{\mathbf{r}}, t) = \frac{1}{\sqrt{\pi}} \int_{-\infty}^{t} \frac{d\tau}{(t-\tau)^{3/2}} e^{-\frac{\tilde{r}^2}{t-\tau}} \left\{e^{-\frac{|\mathbf{x}'(\tau,t)|^2}{t-\tau}} e^{-\frac{2\mathbf{x}'(\tau,t)\cdot\tilde{\mathbf{r}}}{t-\tau}} - e^{-(t-\tau)v^2(t)} e^{-2\mathbf{v}(t)\cdot\tilde{\mathbf{r}}}\right\}. \tag{4.13}$$

Under rather mild conditions on the particle motion, discussed below, it is justified to naively expand the integrand in Eq. (4.13) as $\tilde{r} \searrow 0$ and integrate term by term to find

$$\Delta\tilde{c}_1(\tilde{\mathbf{r}}, t) = h[\mathbf{v}](t) + \tilde{\mathbf{r}}\cdot\mathbf{H}[\mathbf{v}](t) + o(\tilde{r}) \quad \text{as} \quad \tilde{r} \searrow 0, \tag{4.14}$$

where we define the functionals

$$h[\mathbf{v}](t) = \frac{1}{\sqrt{\pi}} \int_{-\infty}^{t} \frac{d\tau}{(t-\tau)^{3/2}} \left\{e^{-\frac{|\mathbf{x}'(\tau,t)|^2}{t-\tau}} - e^{-(t-\tau)v^2(t)}\right\} \tag{4.15}$$

and

$$\mathbf{H}[\mathbf{v}](t) = \frac{2}{\sqrt{\pi}} \int_{-\infty}^{t} \frac{d\tau}{(t-\tau)^{5/2}} \left\{(t-\tau)\mathbf{v}(t)e^{-(t-\tau)v^2(t)} - \mathbf{x}'(\tau,t)e^{-\frac{|\mathbf{x}'(\tau,t)|^2}{t-\tau}}\right\}. \tag{4.16}$$

Substituting the local expansions (4.11) and (4.14) into the decomposition (4.10) gives the local expansion of the remote-region concentration $\tilde{c}_1(\tilde{\mathbf{r}}, t)$ as $\tilde{r} \searrow 0$ to order $\tilde{r}$. Comparing that expansion with Eq. (3.13) gives $\tilde{h}(t) = -2v(t) + h[\mathbf{v}](t)$ and, more importantly,

$$\tilde{\mathbf{H}}(t) = 4v(t)\mathbf{v}(t) + \mathbf{H}[\mathbf{v}](t). \tag{4.17}$$

We shall refer to $\mathbf{H}[\mathbf{v}](t)$ as the history operator, with the notation $[\mathbf{v}](t)$ indicating a functional dependence upon $\mathbf{v}(\tau)$ over past times $\tau \leqslant t$. In equations where the dependence on t is implicit, we shall still indicate the functional dependence by writing $\mathbf{H}[\mathbf{v}]$. The history operator clearly vanishes for steady rectilinear motion. Hence, Eq. (4.17) decomposes the vector quantity $\tilde{\mathbf{H}}(t)$ into quasisteady and inherently unsteady parts.

A subtle point is that the definition of $\tilde{\mathbf{H}}(t)$ via the remote-region initial-boundary-value problem (cf. Sec. III C) is slightly more general than that based on the decomposition (4.17) and the history

operator (4.16). Indeed, the singular integral in Eq. (4.16) converges only if $\mathbf{x}'(\tau,t)=\mathbf{v}(t)(t-\tau)+\mathcal{O}[(t-\tau)^q]$ as $\tau\nearrow t$, with $q>3/2$. [This condition is actually necessary for justifying the straightforward expansion of Eq. (4.13) leading to Eq. (4.14).] With reference to Eq. (4.9), this condition is clearly satisfied for any smooth particle trajectory, in which case $q\geqslant 2$. We will also consider scenarios involving a force discontinuity, say at time $t=t_0$, in which case we shall find that $\mathbf{v}(t)$ is continuous but varies like $(t-t_0)^{1/2}$ as $t\searrow t_0$. The above condition on $\mathbf{x}'(\tau,t)$ still holds as the left derivative of $\mathbf{v}(t)$ exists at any fixed t including t_0.

C. Slowly varying velocity

If $\mathbf{v}(t)$ varies slowly enough, the history operator can sometimes be expanded in terms of differential operators, as follows. The first term in the integrand in Eq. (4.16) attenuates exponentially over the recent history $t-\tau=\mathcal{O}(1/v^2(t))$. If $\mathbf{v}(t)$ is nonvanishing and varies on a timescale $T\gg 1/v^2$, then considering the "recent history" $t-\tau=\mathcal{O}[1/v^2(t)]$, we can expand

$$\mathbf{x}'(\tau,t)=\int_\tau^t ds\,\mathbf{v}(s)=(t-\tau)\mathbf{v}-\frac{1}{2}(t-\tau)^2\dot{\mathbf{v}}+\frac{1}{6}(t-\tau)^3\ddot{\mathbf{v}}+\cdots, \tag{4.18}$$

with each subsequent term being $1/(v^2T)$ smaller in order of magnitude. (An upper dot denotes differentiation with respect to t, with the velocity $\mathbf{v}$ and its derivatives evaluated at time t unless stated otherwise.) Furthermore, in the same interval we have the expansion

$$e^{-\frac{|\mathbf{x}'(\tau,t)|^2}{t-\tau}}=e^{-(t-\tau)v^2}\left\{1+(t-\tau)^2\dot{\mathbf{v}}\cdot\mathbf{v}+\left[\frac{1}{2}(t-\tau)^4(\dot{\mathbf{v}}\cdot\mathbf{v})^2-(t-\tau)^3\left(\frac{|\dot{\mathbf{v}}|^2}{4}+\frac{\ddot{\mathbf{v}}\cdot\mathbf{v}}{3}\right)\right]+\cdots\right\}. \tag{4.19}$$

It is therefore clear that the second term in the integrand in Eq. (4.16) attenuates exponentially on the same timescale as the first, whereby the contribution of the recent history is local. Thus, substituting Eqs. (4.18) and (4.19) into Eq. (4.16) and integrating term by term yields

$$\mathbf{H}[\mathbf{v}]=\frac{\mathsf{I}-\hat{\mathbf{v}}\hat{\mathbf{v}}}{v}\cdot\dot{\mathbf{v}}+\left[3\frac{|\dot{\mathbf{v}}|^2\hat{\mathbf{v}}-5(\hat{\mathbf{v}}\cdot\dot{\mathbf{v}})^2\hat{\mathbf{v}}+2(\hat{\mathbf{v}}\cdot\dot{\mathbf{v}})\dot{\mathbf{v}}}{8v^4}-\frac{(\mathsf{I}-3\hat{\mathbf{v}}\hat{\mathbf{v}})\cdot\ddot{\mathbf{v}}}{6v^3}\right]+\cdots, \tag{4.20}$$

wherein $\hat{\mathbf{v}}=\mathbf{v}/v$.

Besides the condition that $\mathbf{v}(t)$ varies sufficiently slowly, the expansion (4.20) can fail in situations where the particle returns to a location it has already visited. This is because $\mathbf{x}'(\tau,t)$ is small near those past moments and hence there can be localized contributions to the integral in Eq. (4.16) from the nonrecent history that are only algebraically small.

D. Linearization

We next consider the linearization of the history operator about either the stationary state or steady rectilinear motion. Writing $\mathbf{v}(t)=\mathbf{v}_0+\delta\mathbf{v}(t)$, wherein $\mathbf{v}_0$ is a constant vector (possibly the zero vector) of magnitude v_0 and direction $\hat{\mathbf{v}}_0$, and $\delta\mathbf{v}(t)$ a perturbation, we find from Eq. (4.16) that, to linear order in the perturbation,

$$\mathbf{H}[\mathbf{v}]=\delta\mathbf{H}[\delta\mathbf{v};\mathbf{v}_0], \tag{4.21}$$

where

$$\delta\mathbf{H}[\delta\mathbf{v};\mathbf{v}_0]=\frac{2}{\sqrt{\pi}}\int_{-\infty}^t d\tau\,\frac{e^{-(t-\tau)v_0^2}}{(t-\tau)^{5/2}}\{\mathsf{I}-2(t-\tau)\mathbf{v}_0\mathbf{v}_0\}\cdot\int_\tau^t ds\,\{\delta\mathbf{v}(t)-\delta\mathbf{v}(s)\}. \tag{4.22}$$

For linearization about the stationary state, we set $\mathbf{v}_0=\mathbf{0}$. In that case, interchanging the order of integration in Eq. (4.22) and performing the integration in τ gives

$$\delta\mathbf{H}[\delta\mathbf{v};\mathbf{0}]=\frac{4}{3\sqrt{\pi}}\int_{-\infty}^t ds\,\frac{\delta\mathbf{v}(t)-\delta\mathbf{v}(s)}{(t-s)^{3/2}}. \tag{4.23}$$

We note that this linearization fails for a perturbation that decayed too fast in the far past, since with the integrand in Eq. (4.23) behaving like $\delta\mathbf{v}(s)/|s|^{3/2}$ as $s \to -\infty$ the contribution of the far past could diverge. In particular, this linearization can describe exponentially growing but not exponentially decaying perturbations. Thus, assuming an exponential perturbation of the form $\delta\mathbf{v}(t) = \mathbf{A}e^{\sigma t}$, wherein $\mathbf{A}$ is a constant vector and σ a complex growth rate, Eq. (4.23) gives

$$\delta\mathbf{H}[\mathbf{A}e^{\sigma t};\mathbf{0}] = \tfrac{8}{3}\sigma^{1/2}\mathbf{A}e^{\sigma t} \tag{4.24}$$

for $\operatorname{Re}\sigma \geqslant 0$, where the square root takes its principal value.

For linearization about a steady rectilinear motion, we have $v_0 \neq 0$. In that case, interchanging the order of integration in Eq. (4.22) and performing the integration in τ gives, after making the change of variables $q = v_0^2(t-s)$,

$$\delta\mathbf{H}[\delta\mathbf{v};\mathbf{v}_0] = \frac{2v_0}{\sqrt{\pi}}\int_0^\infty dq\,\{\mathsf{I}f_1(q) - 2\hat{\mathbf{v}}_0\hat{\mathbf{v}}_0 f_2(q)\}\cdot\left\{\delta\mathbf{v}(t) - \delta\mathbf{v}\left(t - q/v_0^2\right)\right\}, \tag{4.25}$$

in which

$$f_1(q) = \frac{2(1-2q)e^{-q}}{3q^{3/2}} + \frac{4\sqrt{\pi}}{3}\operatorname{erfc}(q^{1/2}), \tag{4.26a}$$

$$f_2(q) = 2q^{-1/2}e^{-q} - 2\sqrt{\pi}\operatorname{erfc}(q^{1/2}), \tag{4.26b}$$

with erfc the complementary error function [19]. As $q \to 0$, $f_1(q)$ and $f_2(q)$ scale like $q^{-3/2}$ and $q^{-1/2}$, respectively; this confirms that the integration in Eq. (4.25) converges as $q \to 0$, as the second curly bracket on the right-hand side of Eq. (4.26) scales like q in that limit. As $q \to \infty$, these functions scale like $q^{-5/2}e^{-q}$ and $q^{-3/2}e^{-q}$. Hence, the linearization about a steady rectilinear motion fails for perturbations that decay at a too high exponential rate in the far past. Assuming an exponential perturbation as before, we find from Eq. (4.25)

$$\delta\mathbf{H}[\mathbf{A}e^{\sigma t};\mathbf{v}_0] = \frac{8v_0}{3\sigma'}\left\{\mathsf{I}\left[(1+\sigma')^{3/2} - 1 - \frac{3}{2}\sigma'\right] - \frac{3}{2}\hat{\mathbf{v}}_0\hat{\mathbf{v}}_0[(1+\sigma')^{1/2} - 1]^2\right\}\cdot\mathbf{A}e^{\sigma t}, \tag{4.27}$$

for $\operatorname{Re}\sigma' \geqslant -1$, wherein $\sigma' = \sigma/v_0^2$. We note that Eq. (4.27) degenerates to Eq. (4.24) as $v_0 \to 0$ and agrees with a linearization of the slowly varying approximation (4.19) in the limit $\sigma \to 0$.

V. HISTORY-DEPENDENT DYNAMICS

A. Weakly nonlinear model and numerical method

Let us recapitulate the weakly nonlinear model we have developed for the slow dynamics of a force-free or weakly forced isotropic active particle near the threshold for spontaneous motion. Recall the definition $\mathrm{Pe} = 4 + \epsilon\chi$, with $0 < \epsilon \ll 1$ and χ a rescaled bifurcation parameter, and that the slow time t is normalized by $a_*/(\epsilon^2 u_*)$. The particle velocity $\mathbf{v}(t)$ in the laboratory frame (normalized by ϵu_*) satisfies the unsteady amplitude equation [cf. Eqs. (3.24) and (4.17)] gives

$$(\chi - 16v)\mathbf{v} - 4\mathbf{H}[\mathbf{v}] + 2\mathbf{f} = \mathbf{0}, \tag{5.1}$$

where $v(t)$ is the magnitude of $\mathbf{v}(t)$, $\mathbf{f}(t)$ is the generally time-dependent force on the particle (normalized by $6\pi\epsilon^2\eta_* u_* a_*$) and the history operator is given by

$$\mathbf{H}[\mathbf{v}](t) = \frac{2}{\sqrt{\pi}}\int_{-\infty}^{t}\frac{d\tau}{(t-\tau)^{5/2}}\left\{(t-\tau)\mathbf{v}(t)e^{-(t-\tau)v^2(t)} - \mathbf{x}'(\tau,t)e^{-\frac{|\mathbf{x}'(\tau,t)|^2}{t-\tau}}\right\}, \tag{5.2}$$

in which

$$\mathbf{x}'(\tau,t) = \mathbf{x}(t) - \mathbf{x}(\tau) = \int_\tau^t \mathrm{d}s\,\mathbf{v}(s) \tag{5.3}$$

is the position of the particle (normalized by a_*/ϵ) at time t measured from the position at the past time τ, with $\mathbf{x}(t)$ being the position of the particle measured from a fixed point in the laboratory frame (see Fig. 3). The history operator $\mathbf{H}[\mathbf{v}](t)$ captures the relaxation of the particle's concentration wake, vanishing for a constant particle velocity in which case the wake is steady in a comoving frame.

We call attention to the fact that only the product $\epsilon\chi$, in which ϵ is constrained to be positive, has physical significance, rather than ϵ or χ separately. We could generally choose $\chi = \pm 1$, in which case ϵ is the absolute magnitude of Pe $-$ 4 and the magnitude of the force is characterized by that of $\mathbf{f}(t)$. A different viewpoint is that ϵ^2 characterizes the magnitude of the force, in which case χ is a free parameter.

For the remainder of this section we study the above weakly nonlinear model both analytically and numerically. In Sec. V B, we review its steady-state solutions, already known from part I and earlier works [8–10]. In Sec. V C we analyze the stability of those steady states by employing the linearization of the history operator developed in Sec. IV D, and illustrate the results via numerical simulations. In Sec. V D, we study the alignment dynamics of a spontaneously moving particle following the sudden application of an external force, supplementing numerical simulations with analytical approximations based on the expansion developed in Sec. IV C of the history operator for a slowly varying particle velocity.

For the numerical simulations, we assume that $\mathbf{v}(t)$ is known and constant for $t < 0$, corresponding to a steady state of Eq. (5.1) for some constant forcing. The main step in the numerical scheme takes a sequence of values $\mathbf{x}(t_i)$ at (adaptable) times $t_0 = 0, t_1, \ldots, t_{n-1}$ and calculates the value $\mathbf{x}(t_n)$ using Newton iteration. The history operator is evaluated using the analytical expressions derived in Appendix B 1 for the prescribed "tail" $\tau < 0$ and the trapezoidal rule for $0 \leqslant \tau < t$. For the latter integration, we use either the basic form (5.2) of the history operator where the integrand exhibits an integrable $1/(t-\tau)^{1/2}$ singularity as $\tau \nearrow t$, which requires estimating the velocity $\mathbf{v}(t_n)$, or a regularized version of the history operator developed in Appendix C, which requires estimating also the acceleration $\mathbf{a}(t_n) = (d\mathbf{v}/dt)(t_n)$; the regularization improves the order of the scheme from $\mathcal{O}(\Delta t^{1/2})$ to $\mathcal{O}(\Delta t^{3/2})$, wherein Δt is the time step. We generally assume that $\mathbf{f}(t)$ is smooth but the code does allow for discontinuity at $t = 0$; in that case, we employ the early-time asymptotic expansion derived in Appendix B 2 to determine the values of $\mathbf{x}(t_i)$ for the first few initial times.

B. Steady-state solutions

We look for steady state solutions $\mathbf{v}(t) = \bar{\mathbf{v}}$ of the amplitude equation (5.1), of magnitude $\bar{v}$ and direction $\hat{\bar{\mathbf{v}}}$. For this purpose, we assume a constant force $\mathbf{f}(t) = f\hat{\boldsymbol{\imath}}$, with $f \geqslant 0$ and $\hat{\boldsymbol{\imath}}$ a unit vector. As the history operator $\mathbf{H}[\mathbf{v}](t)$ vanishes for a constant velocity, Eq. (5.1) reduces to the steady amplitude equation

$$(\chi - 16\bar{v})\bar{\mathbf{v}} + 2f\hat{\boldsymbol{\imath}} = \mathbf{0}, \tag{5.4}$$

which was already derived and studied in part I. It was also derived in Ref. [10] with the *a priori* assumption that the motion is collinear with the force, and earlier in Refs. [6,7] for a closely related active-drop model.

Consider first the case $f = 0$ corresponding to a freely suspended particle. For all χ, we find the trivial steady state $\bar{\mathbf{v}} = \mathbf{0}$. Additionally, for $\chi > 0$ we find nontrivial steady states corresponding to spontaneous rectilinear motion with speed $\bar{v} = \chi/16$ and arbitrary direction.

Consider next the case $f > 0$ corresponding to a constant external force. In contrast to the force-free case, where the direction of steady spontaneous motion is arbitrary, it is evident from Eq. (5.4) that in the forced case steady motion is necessarily collinear with the force no matter the force magnitude. We accordingly write $\bar{\mathbf{v}} = \bar{v}_\parallel\hat{\boldsymbol{\imath}}$, with the component $\bar{v}_\parallel$ found to satisfy the bifurcation relation

$$\chi\bar{v}_\parallel - 16|\bar{v}_\parallel|\bar{v}_\parallel + 2f = 0. \tag{5.5}$$

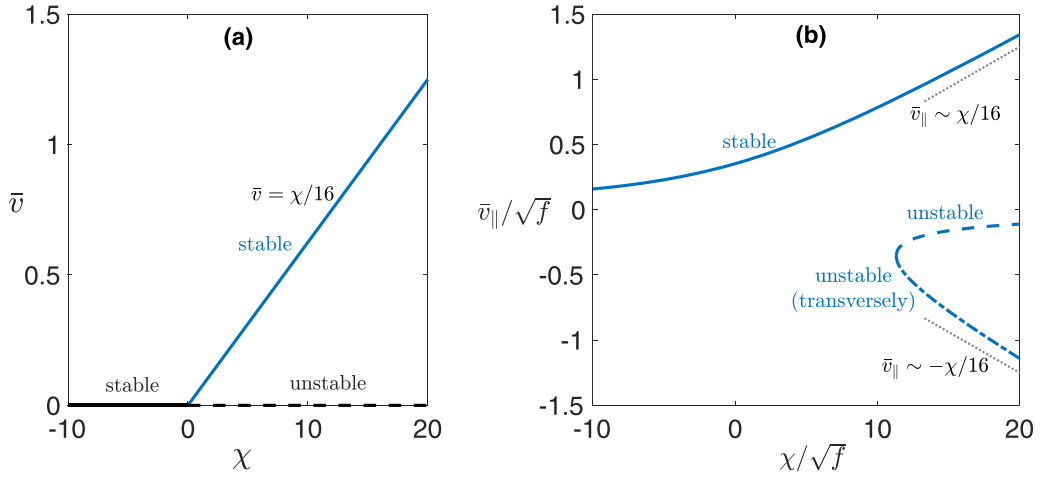

FIG. 4. Steady bifurcation diagrams for a freely suspended (a) and forced (b) active particle, as found in Sec. V B. The indicated stability characteristics are deduced in Sec. V C.

For all χ, we find the parallel ($\bar{v}_\parallel > 0$) branch

$$v_\parallel = \frac{1}{32}(\chi + \sqrt{\chi^2 + 128f}). \tag{5.6}$$

For $\chi > 8\sqrt{2f}$, we additionally find the two antiparallel ($\bar{v}_\parallel < 0$) branches

$$v_\parallel = -\frac{1}{32}(\chi \pm \sqrt{\chi^2 - 128f}), \tag{5.7}$$

which are degenerate at $\chi = 8\sqrt{2f}$.

Steady bifurcation diagrams in the free and forced cases are depicted in Fig. 4. Clearly in the latter case the dependence on f can be scaled out by noting that $\bar{v}_\parallel/\sqrt{f}$ is a function of $\chi/\sqrt{f}$.

C. Linear stability

We next consider the linear stability of the steady states found above. Upon writing $\mathbf{v}(t) = \bar{\mathbf{v}} + \delta\mathbf{v}(t)$, with $\bar{\mathbf{v}}$ a solution of the steady amplitude equation (5.4) and $\delta\mathbf{v}(t)$ an infinitesimal perturbation, a linearization of the unsteady amplitude equation (5.1)

$$\{\chi - 16\bar{v}(\mathsf{I} + \hat{\bar{\mathbf{v}}}\hat{\bar{\mathbf{v}}})\} \cdot \delta\mathbf{v} - 4\,\delta\mathbf{H}[\delta\mathbf{v}; \bar{\mathbf{v}}] = \mathbf{0}, \tag{5.8}$$

where the linearized history operator $\delta\mathbf{H}[\delta\mathbf{v}; \bar{\mathbf{v}}]$ is provided by Eq. (4.23) for $\bar{\mathbf{v}} = \mathbf{0}$ and Eq. (4.25) for $\bar{\mathbf{v}} \neq \mathbf{0}$. Specifically, we look for exponential solutions of the form $\delta\mathbf{v}(t) = \mathbf{A}e^{\sigma t}$, with $\mathbf{A}$ a constant vector and σ a complex-valued growth rate. We recall from Sec. IV D that the linearization of the history operator is only valid for perturbations that don't decay too quickly; in particular, for exponential solutions of the above form, $\delta\mathbf{H}[\delta\mathbf{v}; \bar{\mathbf{v}}]$ reduces to Eq. (4.24) for $\bar{v} = 0$, requiring $\mathrm{Re}\,\sigma \geqslant 0$, and Eq. (4.27) for $\bar{v} \neq 0$, requiring $\mathrm{Re}\,\sigma \geqslant -\bar{v}^2$. Existence of exponentially growing solutions implies instability, of course. We shall also assume that the absence of either constant or exponentially growing solutions implies stability (if a constant solution is the fastest growing solution then we shall say that the stability is marginal); we discuss this assumption below in Sec. V C 5.

1. Stability of the stationary state in the force-free scenario

Consider first the stationary state that exists for all χ in the unforced case. Substituting Eq. (4.24) into Eq. (5.8) gives exponential perturbations with arbitrary amplitude $\mathbf{A}$ and growth rate σ satisfying

$$\sigma^{1/2} = \frac{3\chi}{32} \tag{5.9}$$

and $\mathrm{Re}\,\sigma \geqslant 0$, with the square root taking its principal value. We accordingly conclude that the stationary state is unstable for $\chi > 0$, marginally stable for $\chi = 0$ and stable for $\chi < 0$.

2. Stability of steady rectilinear-motion states

We next derive general results for $\bar{\mathbf{v}} \neq \mathbf{0}$ which we will subsequently apply to infer the stability of the steady spontaneous-motion states in the force-free and forced scenarios. By substituting Eq. (4.27) into Eq. (5.8), we find the condition

$$\frac{(1+\sigma')^{3/2}-1}{\sigma'} + 3\delta_{\parallel}\frac{(1+\sigma')^{1/2}-1}{\sigma'} = \chi', \tag{5.10}$$

in which

$$\sigma' = \sigma/\bar{v}^2, \quad \chi' = 3\chi/(32\bar{v}),$$

and $\delta_{\parallel}$ equals 1 for longitudinal perturbations $\mathbf{A} \parallel \bar{\mathbf{v}}$ and vanishes for transverse perturbations $\mathbf{A} \perp \bar{\mathbf{v}}$. Recall that in the present case the growth rate must also satisfy $\mathrm{Re}\,\sigma' \geqslant -1$.

For longitudinal perturbations, we find that Eq. (5.10) has no solutions for $\chi' < 1$ and two solutions for $\chi' > 1$, degenerate at $\chi' = 1$, given by

$$\sigma_L'^{\pm} = \tfrac{1}{2}\{\chi'^2 - 9 \pm (\chi'-1)(\chi'-3)^{1/2}(\chi'+5)^{1/2}\}. \tag{5.12}$$

For $1 < \chi' < 3$, the solutions (5.12) are complex conjugate with a negative real part (with $\mathrm{Re}\,\sigma' \geqslant -1$ only at and beyond an intermediate χ'). For $\chi' = 3$, they degenerate to the zero solution. For $\chi' > 3$, there is one positive solution and one negative solution (both with $\mathrm{Re}\,\sigma' \geqslant -1$). We conclude that the spontaneous-motion state is longitudinally unstable for $\chi' > 3$, marginally longitudinally stable for $\chi' = 3$ and longitudinally stable for $\chi' < 3$.

For transverse perturbations, we find that Eq. (5.10) has no solutions for $\chi' < 1$ and just one (real) solution for $\chi' \geqslant 1$ given by

$$\sigma_T' = \tfrac{1}{2}\{\chi'^2 - 3 + (\chi'+3)^{1/2}(\chi'-1)^{3/2}\}. \tag{5.13}$$

This solution is negative for $1 \leqslant \chi' < 3/2$ (between -1 and 0, hence satisfying the condition $\mathrm{Re}\,\sigma' \geqslant -1$), vanishes for $\chi' = 3/2$, and positive for $\chi' > 3/2$. Thus, the spontaneous-motion state is transversely unstable for $\chi' > 3/2$, marginally transversely stable for $\chi' = 3/2$ and transversely stable for $\chi' < 3/2$.

3. Stability of spontaneous motion in the force-free scenario

We next apply the above results to the nontrivial steady solutions of Eq. (5.4). In the unforced scenario, substituting $\bar{v} = \chi/16$ (wherein $\chi > 0$) into Eq. (5.11b) gives $\chi' = 3/2$ [cf. Eq. (5.11b)]. We accordingly conclude that the steady spontaneous-motion states in the force-free case are longitudinally stable and transversely marginally stable. Clearly an infinitesimal transverse perturbation simply leaves the particle velocity in the isotropic manifold of steady states.

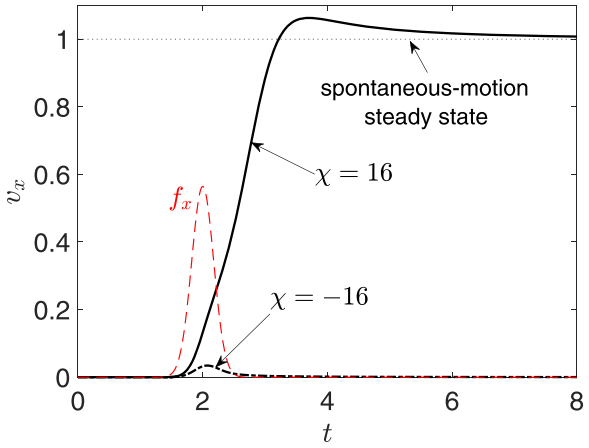

FIG. 5. The dynamical response of an isotropic active particle, initially at rest, to a unidirectional gaussian force input (chosen arbitrarily in the $\hat{\mathbf{e}}_x$ direction). Depending on the sign of χ, the particle is observed to either relax back to its stationary state or to approach a state of steady spontaneous motion in the direction of the force disturbance.

4. Stability of rectilinear motion in the forced scenario

Consider next the forced case. For the parallel state, which exists for all χ and is given by Eq. (5.6), Eq. (5.11b) gives $\chi' = \chi'_P(\chi/\sqrt{f})$, where

$$\chi'_P(x) = \frac{3x}{x + \sqrt{x^2 + 128}}. \tag{5.14}$$

Since $\chi'_P < 3/2$, we conclude that the parallel state is stable. For the antiparallel states, which exist for $\chi > 8\sqrt{2f}$ and are provided by Eq. (5.7), Eq. (5.11b) gives $\chi' = \chi'_{AP,1}(\chi/\sqrt{f})$ for the larger-magnitude branch and $\chi' = \chi'_{AP,2}(\chi/\sqrt{f})$ for the smaller-magnitude branch, where

$$\chi'_{AP,1}(x) = \frac{3x}{x + \sqrt{x^2 - 128}}, \quad \chi'_{AP,2}(x) = \frac{3x}{x - \sqrt{x^2 - 128}}. \tag{5.15a,b,c}$$

Since $3/2 < \chi'_{AP,1} < 3$ the larger-magnitude antiparallel state is longitudinally stable but transversely unstable, so overall unstable. Furthermore, since $\chi'_{AP,2} > 3$ the smaller-magnitude antiparallel is unstable (both longitudinally and transversely).

5. Discussion and numerical demonstrations

Let us summarize the above stability results, which we have indicated in the steady bifurcation diagrams in Fig. 4. In the unforced case, the stationary state is unstable for $\chi > 0$, while the spontaneous-motion states are longitudinally stable and transversely marginally stable (as a transverse perturbation leaves the particle velocity in the isotropic manifold of spontaneous-motion states). In the forced case, the parallel state is stable; while both antiparallel states are unstable, the larger-magnitude antiparallel state is longitudinally stable.

To test our stability predictions, in Figs. 5–7 we numerically simulate particles that are disturbed from steady-state motion (force-free or forced) by finite localized (Gaussian) force perturbations. We find that our predictions qualitatively agree with the observed dynamics in all cases.

It is useful to compare our stability predictions with related results in the literature. The main stability result in the literature is the linear-stability analysis of Michelin *et al.* of the stationary state [1], starting from the full model as formulated in Sec. II in the case where there is no force.

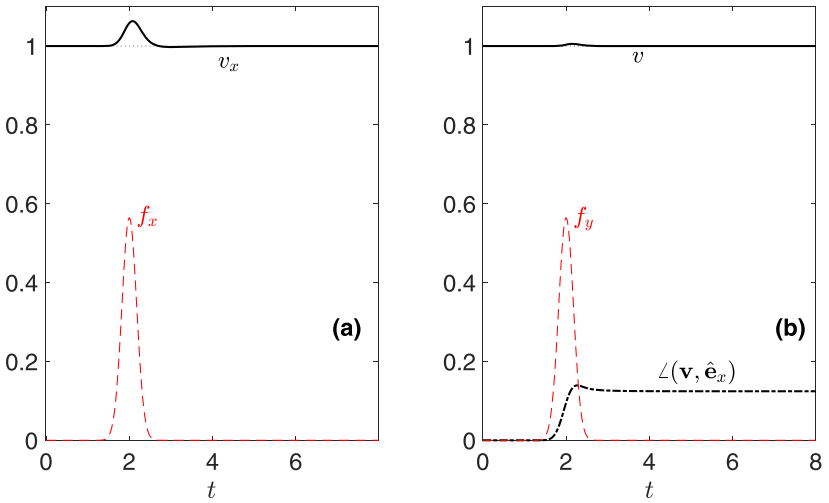

FIG. 6. The dynamical response of an isotropic active particle at $\chi = 16$, initially at the steady spontaneous-motion state $\bar{\mathbf{v}} = \hat{\mathbf{e}}_x$, to a unidirectional gaussian force input either in the longitudinal $\hat{\mathbf{e}}_x$ direction (a) or a transverse direction (b), the latter chosen arbitrarily as the $\hat{\mathbf{e}}_y$ direction. In (a) the particle velocity $\mathbf{v}(t) = v_x(t)\hat{\mathbf{e}}_x$ relaxes back to its initial spontaneous-motion state. In (b) the particle speed v relaxes back to its initial value but the direction of motion at long times differs from the initial one, namely the particle settles into spontaneous motion in a different direction.

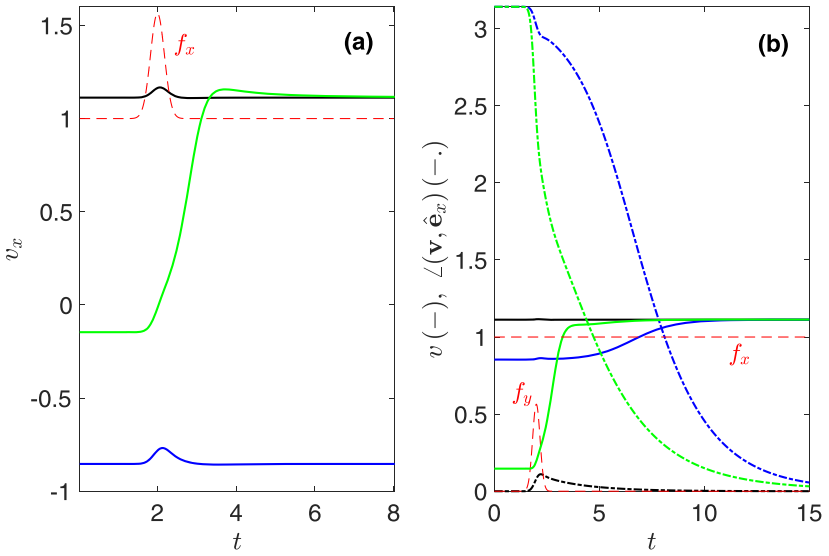

FIG. 7. An isotropic active particle at $\chi = 16$ is initially at a steady state $\bar{\mathbf{v}} = \bar{v}_\parallel \hat{\mathbf{e}}_x$ corresponding to a constant force $\mathbf{f} = \hat{\mathbf{e}}_x$ (black: parallel state, blue: larger-magnitude antiparallel state, green: smaller-magnitude antiparallel state). We show the dynamical response to a unidirectional gaussian force-disturbance input (dashed red curves) either in the longitudinal $\hat{\mathbf{e}}_x$ direction (a) or a transverse direction (b), the latter chosen arbitrarily as the $\hat{\mathbf{e}}_y$ direction. In (a) the particle velocity $\mathbf{v}(t) = v_x(t)\hat{\mathbf{e}}_x$; the component $v_x(t)$ (solid curves) is seen to relax back to its initial value for the parallel and larger-magnitude antiparallel states, and to approach the value corresponding to the parallel state for the smaller-magnitude antiparallel state. In (b) the particle approaches the parallel state in all cases; in particular, the speed $v(t)$ approaches its corresponding steady state (solid curves) and the angle between $\mathbf{v}(t)$ and $\hat{\mathbf{e}}_x$ attenuates (dash-dotted curves).

(A generalization of this stability analysis to a closely related model of an active drop is given in Ref. [8].) They look for exponential solutions and find that all growth-rate eigenvalues are real. In particular, they find that exponential solutions with a positive growth rate exist for $\mathrm{Pe} > 4$, in agreement with our finding that the stationary state is unstable for $\chi > 0$. Moreover, we find that their implicit solution for positive growth rates [Eq. (14) therein] degenerates to our solution (5.9) as $\mathrm{Pe} \searrow 4$. As further discussed below, they also find that for all Péclet numbers any negative growth rate is possible.

We are not aware of a comparable linear-stability analysis in the literature for the rectilinear-motion states in either the force-free or forced cases. In the force-free case, it is natural to simply assume that the spontaneous-motion states are stable (at least in some interval of Péclet numbers above the threshold). We note that in Appendix B of Ref. [9] the authors claim to confirm the linear stability of the spontaneous-motion state for a closely related model of an active drop, but their calculation appears to rely on an axisymmetric weakly nonlinear analysis that incorrectly neglects the history effect.

In the forced case, it has been incorrectly guessed in Ref. [10] that both the parallel and larger-magnitude antiparallel states are stable, while the smaller-magnitude antiparallel state is unstable (we have shown that the larger-magnitude antiparallel state is transversely unstable). This claim has been referenced in a recent review on active drops [4] and in a recent axisymmetric numerical study [13]. We note that earlier weakly nonlinear analyses of forced active drops have concluded similar to here that there is a stable parallel state and, in some cases, also two unstable antiparallel states. In Refs. [6,7], where the active-drop model is closely related to our particle formulation, only a heuristic relative-stability argument is given which is strictly based on calculating steady states. In Ref. [20], this conclusion is reached based on an unsteady weakly nonlinear analysis, but for an active-drop model that does not involve bulk transport and hence differs fundamentally from our particle model in that there is no history effect.

Finally, we discuss the limitations of our linear stability analysis, within the framework of the weakly nonlinear model. First, we have assumed above that if the growth-rate equation (5.9) or (5.10) does not have a solution with positive real part then all perturbations decay, but this does not reveal the rate of decay in the cases where there is no solution at all. To analyze the general evolution of linear perturbations with time, we can consider the response of the particle to a force impulse (i.e., similar to the numerical demonstrations in Figs. 5–7 but with infinitesimal localized perturbations). In Appendix D, we perform this analysis using Laplace transforms and contour deformation, and show that if the equations do not have a solution satisfying the necessary condition $\mathrm{Re}\,\sigma \geqslant -\bar{v}^2$, then the linear perturbations decay like $e^{-\bar{v}^2 t}$ times a power of t as $t \to \infty$. In particular, for linearization about the stationary state we find that the decay of perturbations for $\chi < 0$ is algebraic.

Second, the formulation with the history operator (4.17) assumes that the perturbations to the concentration field are solely generated by perturbations to the particle motion. To consider more general perturbations to the concentration field, one would have to employ the amplitude equation in the form (3.24), with $\tilde{\mathbf{H}}(t)$ defined by the unsteady remote-region concentration problem of Sec. III C rather than the history operator via Eq. (4.17). While we do not present this analysis here, we note that using this approach to seek perturbations with time dependence $e^{\sigma t}$ to the stationary state in the force-free case recovers the result (5.10) for $\chi > 0$, while for $\chi < 0$ any negative growth rate is possible, by an appropriate choice of the initial concentration distribution, which is in agreement with the findings in Ref. [1].

D. Alignment dynamics

Consider next an isotropic active particle subjected to the external force $\mathbf{f}(t) = f\mathcal{H}(t)\hat{\boldsymbol{\imath}}$, where $f > 0$ is the force magnitude, $\mathcal{H}(t)$ is the unit-step function and $\hat{\boldsymbol{\imath}}$ is a fixed unit vector. For $t < 0$, the particle can be assumed to be either stationary or, for $\chi > 0$, in a steady spontaneous state moving with speed $\chi/16$ in some direction. The motion is clearly confined to the plane spanned by the force

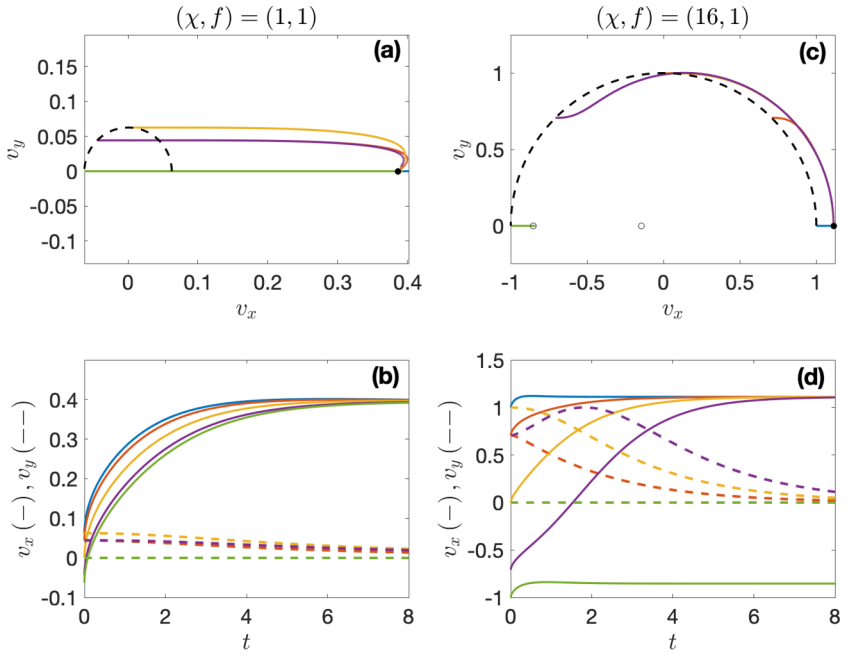

FIG. 8. Dynamical alignment of an isotropic active particle initially at a steady-spontaneous state $\bar{\mathbf{v}} = (\chi/16)\hat{\mathbf{p}}$ with some direction $\hat{\mathbf{p}}$, subjected to a unit-step force in the $\hat{\mathbf{e}}_x$ direction. We take $\chi = 1$ (a), (b) or $\chi = 16$ (c), (d) and choose several $\hat{\mathbf{p}}$ in the x-y plane (distinguished by color) such that $\mathbf{v}(t) = v_x(t)\hat{\mathbf{e}}_x + v_y(t)\hat{\mathbf{e}}_y$. In (a), (c) we plot the path in the v_x-v_y plane; the black dashed semi-circles correspond to the unforced spontaneous-motion steady states, while the solid and hollow circular symbols respectively correspond to stable and unstable steady states with the force on. In (b), (d) we plot the velocity components $v_x(t)$ (solid curves) and $v_y(t)$ (dashed curves) against time.

and the initial spontaneous motion; if the particle is initially stationary, then the motion is collinear with the force.

The stability analysis above suggests that typically the particle will approach with time the parallel steady state for a constant force [cf. Eq. (5.6)], which is stable and exists for all χ; if the particle is initially stationary, or if its initial spontaneous motion happens to be collinear with the force, then depending on the initial state and if $\chi > 8\sqrt{2f}$ the terminal state can also be the larger-magnitude antiparallel state [cf. Eq. (5.7)], which is longitudinally stable but transversely unstable.

We demonstrate the alignment dynamics described above in Fig. 8 by running a series of simulations starting from initial spontaneous-motion states in various directions, for $f = 1$ and two values of $\chi = 1$ and 16. For $\chi = 1$, only the parallel steady state exists; to reach that state, the particle accelerates mainly in the direction of the force, with the initial transverse velocity gradually attenuating. For $\chi = 16$, the parallel and the two antiparallel states exist. For initial spontaneous motion collinear with the force, the particle approaches either the parallel or large-magnitude antiparallel states. For initial spontaneous motion that is noncollinear with the force (regardless of the direction), the particle approaches the parallel state while remaining near the manifold $v = \chi/16$ of unforced spontaneous-motion states.

To analyze the latter scenario analytically, it is convenient to consider the limit $\chi \gg 1$ with f fixed. Given our expectation that the particle velocity remains near the manifold of unforced spontaneous-motion states, we scale the velocity as $\mathbf{v}(t) = \chi\mathbf{V}(t)$. We further assume, subject to *a posteriori* confirmation, that $\mathbf{V}(t)$ varies on an order-unity timescale. In that case, we can use

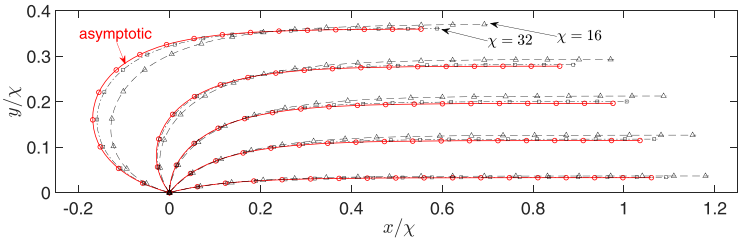

FIG. 9. Dynamical alignment of an isotropic active particle, initially at a steady-spontaneous state $\bar{\mathbf{v}} = (\chi/16)\hat{\mathbf{p}}$ with some direction $\hat{\mathbf{p}}$ in the x-y plane, subjected to a unit-step force in the $\hat{\mathbf{e}}_x$ direction; the simulations are set up such that the particle is at the origin at time $t = 0$ when the force starts to be applied. The black dashed and dash-dotted curves depict numerical simulations of particle position (scaled by χ) for the indicated large values of χ. The red solid curves depict the large-χ (equivalently, weak-force) approximation developed in Sec. V D. The symbols indicate unit time steps.

the "slowly varying" expansion (4.20) of the history operator [the timescale is long compared to $1/v^2 = \mathrm{ord}(1/\chi^2)$] to approximate the unsteady amplitude equation (5.1) as

$$\chi^2(1-16V)\mathbf{V} - \frac{4}{V}\left\{(\mathsf{I}-\hat{\mathbf{V}}\hat{\mathbf{V}})\cdot\frac{d\mathbf{V}}{dt} + \mathcal{O}(\chi^{-4})\right\} + 2f\hat{\boldsymbol{\imath}} = \mathbf{0}. \tag{5.16}$$

We next expand

$$\mathbf{V}(t) \sim \mathbf{V}_0(t) + \chi^{-2}\mathbf{V}_1(t) \quad \text{as} \quad \chi \to +\infty. \tag{5.17}$$

At the leading order χ^2, Eq. (5.16) gives

$$(1-16|\mathbf{V}_0|)\mathbf{V}_0 = \mathbf{0}, \tag{5.18}$$

the general solution being

$$\mathbf{V}_0(t) = \tfrac{1}{16}\hat{\mathbf{P}}(t), \tag{5.19}$$

wherein $\hat{\mathbf{P}}(t)$ is a time-dependent unit vector. Namely, the particle velocity lies on the manifold of unforced spontaneous-motion states, with the direction of motion varying with time. At order unity, Eq. (5.16) gives

$$\frac{d\hat{\mathbf{P}}}{dt} = \frac{1}{2}f\hat{\boldsymbol{\imath}}\cdot(\mathsf{I}-\hat{\mathbf{P}}\hat{\mathbf{P}}), \tag{5.20}$$

where we used the fact that $d\hat{\mathbf{P}}/dt$ is perpendicular to $\hat{\mathbf{P}}$ to eliminate the unknown correction $\mathbf{V}_1(t)$.

The motion is confined to the plane spanned by $\hat{\boldsymbol{\imath}}$ and the initial value of $\hat{\mathbf{P}}$. Let $\vartheta(t) \in (0,\pi)$ be the angle between $\hat{\boldsymbol{\imath}}$ and $\hat{\mathbf{P}}$ and introduce Cartesian coordinates x–y such that $\mathbf{x} = x\hat{\mathbf{e}}_x + y\hat{\mathbf{e}}_y$, with $\hat{\mathbf{e}}_x = \hat{\boldsymbol{\imath}}$ and $\hat{\mathbf{P}} = \cos\vartheta\,\hat{\mathbf{e}}_x + \sin\vartheta\,\hat{\mathbf{e}}_y$. Then Eq. (5.20) becomes

$$\frac{d\vartheta}{dt} = -\frac{f}{2}\sin\vartheta. \tag{5.21}$$

By integrating from an initial angle ϑ_i to a final angle $\vartheta_f < \vartheta_i$ we obtain the alignment time

$$\Delta t \sim \frac{2}{f}\ln\frac{\tan(\vartheta_i/2)}{\tan(\vartheta_f/2)}. \tag{5.22}$$

Furthermore, integrating $d\mathbf{x}/dt \sim \chi \mathbf{V}_0$ using Eqs. (5.19) and (5.21) yields the corresponding Cartesian displacements

$$\Delta x \sim \frac{\chi}{8f} \ln \frac{\sin \vartheta_i}{\sin \vartheta_f}, \tag{5.23a}$$

$$\Delta y \sim \frac{\chi}{8f}(\vartheta_i - \vartheta_f). \tag{5.23b}$$

The approximations (5.22) and (5.23) are illustrated and confirmed against numerical simulations in Fig. 9. While we have derived these approximations for $\chi \to +\infty$ with f fixed, given the partial arbitrariness in the definition of χ they must hold as long as $\chi/\sqrt{f} \gg 1$. Thus for weak force the alignment time is not order unity but long like $1/f$, whereas the displacements scale like χ/f. As to be expected, the alignment time Δt and longitudinal displacement Δx diverge (logarithmically) as either $\vartheta_i \nearrow \pi$ or $\vartheta_f \searrow 0$. In contrast, the transverse displacement Δy limits to $\chi \vartheta_i/(8f)$ as $\vartheta_f \searrow 0$, or $\chi\pi/(8f)$ when also $\vartheta_i \nearrow \pi$.

VI. CONCLUDING REMARKS

Starting from Michelin *et al.*'s canonical model of an isotropic chemically active particle [1], and including the possibility of a weak external force, we employed weakly nonlinear analysis to develop an unsteady, three-dimensional nonlinear amplitude equation (5.1) governing the slow dynamics of the particle valid in the limit where the Péclet number approaches its threshold value for instability and spontaneous motion in the force-free case. An unconventional feature of this unsteady amplitude equation is that it does not explicitly involve time derivatives; rather, unsteadiness enters via a nonlocal term—a time integral over the history of the particle motion representing the interaction of the particle with its own wake (5.2). This manifestation of unsteadiness is a consequence of the spatial nonuniformity of the weakly nonlinear expansion at large distances from the particle. Previously, this same nonuniformity has been linked to other unconventional features of the near-threshold dynamics, including the singular-pitchfork bifurcation in the unperturbed isotropic active-particle scenario and the fact that the amplitude equation arises from solvability at second, rather than third, order of the weakly nonlinear expansion [11].

In contrast to our unsteady theory, previous weakly nonlinear analyses of the canonical active-particle model and closely related models of "self-solubilizing" active drops have either been limited to steady states [6–10] or employed an inconsistent "quasisteady" assumption, as in the weakly nonlinear analysis of axisymmetric drop interaction in Sec. 5 of Ref. [21] and the analysis of the stability of spontaneous-motion states in Appendix B of Ref. [9]. (Unsteady weakly nonlinear analyses of active particles and drops have been carried out before but starting from models of "reactive" active drops where there is no solute transport in the exterior bulk [20], or physically inconsistent active-particle models where solute transport is truncated at a finite distance from the particle [22]; in those cases, the weakly nonlinear expansion is spatially uniform and there is no history effect.) Our unsteady theory can also be related to the "moving singularity" active-drop model proposed in Ref. [23] where wake interaction is included via direct numerical simulation of an unsteady diffusion problem similar to our remote-region problem but with an additional dipolar source term which is meant to capture advection on the particle scale in an ad hoc manner.

We employed our model to analyze and numerically demonstrate the stability characteristics of steady states for both force-free and forced particles. As to be expected from numerical simulations of the canonical active-particle model [1,13,24], in the force-free case we found that above the threshold Péclet value the stationary state loses stability in favor of an isotropic manifold of spontaneous-motion states. In particular, the positive growth rates based on our three-dimensional stability analysis of the stationary state were found to agree asymptotically (approaching the threshold) with the axisymmetric linear stability analysis of the canonical model [1]. In the case of the spontaneous-motion states, there are no stability results in the literature to compare

with. We have shown that these states are stable to longitudinal perturbations, as expected from axisymmetric numerical simulations [1,13]. We also showed that the spontaneous-motion states are only marginally stable to transverse perturbations, since transverse perturbations leave the particle velocity on the manifold of isotropic spontaneous-motion states. Nonlinearly, we observe that a spontaneously moving particle that is transversally perturbed indeed settles back into steady spontaneous motion but in a different direction.

The forced case demonstrates well the need for analyses that are fully three-dimensional (rather than axisymmetric) as well as unsteady. It was previously shown for both active particles [10] and active drops [6,7] that in the presence of a constant force, no matter how weak, steady translation is necessarily collinear with the force. Here, we have shown that the translational steady state parallel to the force that exists for all Péclet numbers (in the vicinity of the threshold) is stable. In contrast, the two antiparallel steady states that exist above a critical Péclet value are both unstable; however, the larger-magnitude antiparallel state is stable under longitudinal perturbations. These findings agree with the heuristic "relative-stability" predictions in Refs. [6,7] for a closely related active-drop model, but contradict the guess made in Ref. [10], later referenced in Refs. [4,13], that the larger-magnitude antiparallel state is stable. Motivated by the instability of the antiparallel states, we have studied the alignment dynamics of a spontaneously moving particle following the sudden application of a force. In particular, we have derived an analytical description of the alignment in a limit where the effect of the force is weak and the particle velocity approximately traces the isotropic manifold of spontaneous-motion steady states from the force-free case.

The unsteady theory developed herein builds upon the steady theory and adjoint formulation developed in part I of this series [5]. In particular, we used a special case of the general solvability condition derived therein to readily extract the amplitude equation for the particle velocity from the inhomogeneous problem at second order of the particle-scale weakly nonlinear expansion. By circumventing the need to solve that inhomogeneous problem, which is generally not axisymmetric and depends on the details of the scenario being considered, we were able to develop a fully three-dimensional treatment and generalize the analysis in part I to the unsteady case without having to redo most of the quasistatic particle-scale analysis.

As extensively demonstrated in part I in the steady case, the general solvability condition developed therein makes it straightforward to include in the modeling various perturbation effects, which generally have a leading-order effect sufficiently near the instability threshold. While in this part we have only included an external force as a perturbation, it would be natural to employ the general framework of part I in conjunction with the unsteady theory in this part toward exploring the dynamics of active particles in a range of perturbations scenarios. This would be immediate for perturbations that only modify the quasistatic particle-scale region. The perturbations could then be included as demonstrated in part I in the steady case, without any modification to the unsteady analysis of the remote region. This applies to most of the examples in part 1, including the external torque, surface-properties and surface-absorption perturbations. In other scenarios, the unsteady analysis of the remote region may require modification. For instance, we have seen in part I that weak bulk absorption can affect the remote region at leading order. In that scenario, the remote-region diffusion equation would include a reaction term proportional to a Damköhler number characterizing the exponential decay of the concentration deviation and so the significance of history.

The theory developed in this and the preceding part could also be readily applied to study N interacting particles whose dimensionless separation is commensurate with the wake scale $1/\epsilon$. In the laboratory frame, the remote region would describe unsteady diffusion from N moving sources of order-ϵ strength, the dominant mechanism of interaction being the order-ϵ^2 concentration gradient induced on any given particle by the wakes of all other particles. We have seen that for an active particle an order-ϵ^2 concentration gradient influences its leading order-ϵ velocity. In comparison, hydrodynamic interactions are negligible. Flat boundaries could also be included in the modeling using the method of images, simultaneously with other perturbations such as an external force. The only published weakly nonlinear analysis of interacting active particles (see Sec. 5 of

Ref. [21]) is limited to axisymmetric collisions and employs a quasistatic assumption that as already mentioned erroneously overlooks the history effect. This overlook and recent interest in the effects of interactions and boundaries on the motion of active drops [23,25–28] suggests this direction as an important application area for our theory.

Last, recall that our theory is derived from the canonical active-particle model of Michelin *et al.* [1], which describes isotropic autocatalytic colloids but is often adopted as a conventional reference model for self-solubilizing active drops [4]. While autocatalytic colloids can be physically realized [2,3], diffusion of the solute molecules they emit or absorb at their surface is typically too strong to allow for a hydrochemical instability; namely, it is difficult in practice to reach the threshold Péclet number. Clearly, it would be desirable to generalize our theory to self-solubilizing active drops. Since drop deformation is usually negligible in these setups, the main differences are that the concentration surface gradient drives flow via a Marangoni effect rather than a diffusio-osmotic slip effect and that the flow in the drop interior needs to be considered. Since these differences can only affect the details of the particle-scale region, we expect that it would be necessary to update the adjoint formulation developed in part I but not the analysis of the unsteady remote region carried out in this part. In light of the above, we anticipate amplitude equations having the same form as in the active-particle case but with different values of the coefficients.

ACKNOWLEDGMENT

The authors are grateful to Mohit Dalwadi and an anonymous referee for constructive comments and acknowledge the generous support of the Leverhulme Trust through Research Project Grant No. RPG-2021-161.

APPENDIX A: LOCAL ANALYSIS OF UNSTEADY REMOTE PROBLEM

In this Appendix, we carry out a local analysis as $\tilde{r} \searrow 0$ of the unsteady remote-region problem (3.10)–(3.12). From this local analysis, we shall obtain the expansion (3.13) with the quantities $\tilde{h}(t)$ and $\tilde{\mathbf{H}}(t)$ undetermined.

Given the singular condition (3.12), we begin by writing

$$\tilde{c}(\tilde{\mathbf{r}}, t) = \frac{1}{\tilde{r}} + C_0(\tilde{\mathbf{r}}, t), \quad \text{with} \quad C_0(\tilde{\mathbf{r}}, t) = o(1/\tilde{r}) \quad \text{as} \quad \tilde{r} \searrow 0. \tag{A1}$$

Since $1/\tilde{r}$ satisfies Laplace's equation for $\tilde{r} > 0$, the governing partial-differential equation (3.10) gives

$$\frac{\partial C_0}{\partial t} - \mathbf{v} \cdot \tilde{\boldsymbol{\nabla}} \frac{1}{\tilde{r}} - \mathbf{v} \cdot \tilde{\boldsymbol{\nabla}} C_0 = \frac{1}{4} \tilde{\nabla}^2 C_0 \quad \text{for} \quad \tilde{r} > 0. \tag{A2}$$

Given Eq. (A1), it is plausible to assume that

$$\frac{\partial C_0}{\partial t}, \tilde{\boldsymbol{\nabla}} C_0 \ll \frac{1}{\tilde{r}^2} \quad \text{as} \quad \tilde{r} \searrow 0, \tag{A3}$$

in which case the dominant balance of Eq. (A2) is

$$\tilde{\boldsymbol{\nabla}}^2 C_0 \sim -4 \mathbf{v} \cdot \boldsymbol{\nabla} \frac{1}{\tilde{r}} \quad \text{as} \quad \tilde{r} \to 0. \tag{A4}$$

The balance (A4) possesses the particular solution

$$-2 \hat{\mathbf{e}}_r \cdot \mathbf{v}. \tag{A5}$$

The only asymptotically consistent homogeneous solutions of Eq. (A4), namely solutions of Laplace's equation in $\tilde{r} > 0$, are constant in space or harmonics increasing with $\tilde{r}$, the former dominating the latter as $\tilde{r} \searrow 0$. We conclude that

$$C_0(\tilde{\mathbf{r}}, t) = \tilde{h}(t) - 2 \hat{\mathbf{e}}_r \cdot \mathbf{v}(t) + C_1(\tilde{\mathbf{r}}, t), \tag{A6}$$

where $\tilde{h}(t)$ is constant in space and $C_1(\tilde{\mathbf{r}}, t) = o(1)$ as $\tilde{r} \to 0$.

Using Eq. (A6) in Eq. (A2), we find

$$\frac{d\tilde{h}}{dt} - 2\hat{\mathbf{e}}_r \cdot \frac{d\mathbf{v}}{dt} + \frac{\partial C_1}{\partial t} + 2\mathbf{v} \cdot \tilde{\boldsymbol{\nabla}}(\hat{\mathbf{e}}_r \cdot \mathbf{v}) - \mathbf{v} \cdot \tilde{\boldsymbol{\nabla}} C_1 = \frac{1}{4}\tilde{\nabla}^2 C_1 \quad \text{for } \tilde{r} > 0. \tag{A7}$$

Making the plausible assumption that $\tilde{\boldsymbol{\nabla}} C_1 \ll 1/\tilde{r}$ as $\tilde{r} \searrow 0$, the left-hand side of Eq. (A7) is dominated by the order-$1/\tilde{r}$ fourth term. Simplifying that term, we find the dominant balance

$$\tilde{\nabla}^2 C_1 \sim \frac{8}{\tilde{r}} \mathbf{vv} : (\mathsf{I} - \hat{\mathbf{e}}_r \hat{\mathbf{e}}_r) \quad \text{as } \tilde{r} \searrow 0. \tag{A8}$$

The balance (A8) possesses the particular solution

$$2\tilde{r}\mathbf{vv} : (\mathsf{I} + \hat{\mathbf{e}}_r \hat{\mathbf{e}}_r). \tag{A9}$$

The only asymptotically consistent homogeneous solutions to Eq. (A8) are growing harmonics, the dominant of which can be written as $\tilde{\mathbf{H}} \cdot \mathbf{X}$, with $\tilde{\mathbf{H}}$ a spatially constant vector. We therefore obtain the local expansion

$$\tilde{c} = \frac{1}{\tilde{r}} + \tilde{h}(t) - 2\mathbf{v} \cdot \hat{\mathbf{e}}_r + \tilde{r}\{2\mathbf{vv} : (\mathsf{I} + \hat{\mathbf{e}}_r \hat{\mathbf{e}}_r) + \tilde{\mathbf{H}}(t) \cdot \hat{\mathbf{e}}_r\} + o(\tilde{r}) \quad \text{as } \tilde{r} \searrow 0, \tag{A10}$$

which is the same as Eq. (3.13) in the main text.

APPENDIX B: STEADY MOTION FOR $t < 0$

1. Analytical integration over the history operator's tail

Consider the scenario where $\mathbf{v}(t) = \bar{\mathbf{v}}$ for $t < 0$, where $\bar{\mathbf{v}}$ is a steady state (magnitude $\bar{v}$) for some constant force $\mathbf{f}_-$ such that [cf. Eq. (5.1)]

$$(\chi - 16\bar{v})\bar{\mathbf{v}} + 2\mathbf{f}_- = \mathbf{0}. \tag{B1}$$

For $t > 0$, we split the history operator (4.16) as

$$\mathbf{H}[\mathbf{v}](t) = \mathbf{H}^-[\mathbf{v}(\tau)]_{\tau=0}^{t}(t;\bar{\mathbf{v}}) + \mathbf{H}^+[\mathbf{v}(\tau)]_{\tau=0}^{t}(t;\bar{\mathbf{v}}), \tag{B2}$$

where the "tail" contribution from past times $\tau < 0$ is

$$\mathbf{H}^-[\mathbf{v}(\tau)]_{\tau=0}^{t}(t;\bar{\mathbf{v}}) = \frac{2}{\sqrt{\pi}} \int_{-\infty}^{0} \frac{d\tau}{(t-\tau)^{5/2}} \left\{ (t-\tau)\mathbf{v}(t) e^{-(t-\tau)v^2(t)} - \mathbf{x}'(\tau,t) e^{-\frac{|\mathbf{x}'(\tau,t)|^2}{t-\tau}} \right\}, \tag{B3}$$

and the contribution from positive past times $0 < \tau < t$ is

$$\mathbf{H}^+[\mathbf{v}(\tau)]_{\tau=0}^{t}(t;\bar{\mathbf{v}}) = \frac{2}{\sqrt{\pi}} \int_{0}^{t} \frac{d\tau}{(t-\tau)^{5/2}} \left\{ (t-\tau)\mathbf{v}(t) e^{-(t-\tau)v^2(t)} - \mathbf{x}'(\tau,t) e^{-\frac{|\mathbf{x}'(\tau,t)|^2}{t-\tau}} \right\}. \tag{B4}$$

We wish to analytically evaluate the tail contribution.

Recalling the definition (4.9), we have

$$\mathbf{x}'(\tau,t) = \mathbf{x}(t) - \mathbf{x}(0) - \tau\bar{\mathbf{v}}, \tag{B5}$$

and so

$$\frac{\mathbf{x}'(\tau,t) \cdot \mathbf{x}'(\tau,t)}{t-\tau} = \bar{v}^2(t-\tau) + 2\bar{\mathbf{v}} \cdot \delta\mathbf{x}(t) + \frac{\delta x^2(t)}{t-\tau}, \tag{B6}$$

where we define

$$\delta\mathbf{x}(t) = \mathbf{x}(t) - \mathbf{x}(0) - \bar{\mathbf{v}}t \tag{B7}$$

and $\delta x(t) = |\delta \mathbf{x}(t)|$. Upon making the change of variables $p = t - \tau$, Eq. (B3) gives, using Eqs. (B5) and (B6),

$$\mathbf{H}^{-}[\mathbf{v}(\tau)]^{t}_{\tau=0}(t;\bar{\mathbf{v}}) = \frac{2\mathbf{v}(t)}{\sqrt{\pi}}\int_t^\infty \frac{dp}{p^{3/2}} e^{-v^2(t)p} - \frac{2}{\sqrt{\pi}} e^{-2\bar{\mathbf{v}}\cdot\delta\mathbf{x}(t)}\left\{\delta\mathbf{x}(t)\int_t^\infty \frac{dp}{p^{5/2}} e^{-\bar{v}^2 p - \delta x^2(t)/p} + \bar{\mathbf{v}}\int_t^\infty \frac{dp}{p^{3/2}} e^{-\bar{v}^2 p - \delta x^2(t)/p}\right\}. \tag{B8}$$

Performing the quadratures, we find

$$\begin{aligned}\mathbf{H}^{-}[\mathbf{v}(\tau)]^{t}_{\tau=0}(t;\bar{\mathbf{v}}) = {} & 4\mathbf{v}(t)\left\{\frac{e^{-tv^2(t)}}{(\pi t)^{1/2}} - v(t)\,\mathrm{erfc}[t^{1/2}v(t)]\right\} \\ & - \frac{2}{\sqrt{\pi}} e^{-2\bar{\mathbf{v}}\cdot\delta\mathbf{x}(t)}\left\{-\frac{\delta\mathbf{x}(t)}{t^{1/2}\delta x^2(t)} e^{-\bar{v}^2 t - \delta x^2(t)/t}\right. \\ & + \frac{\sqrt{\pi}}{4\delta x^3(t)} e^{-2\bar{v}\delta x(t)}[\delta\mathbf{x}(t) + 2\bar{v}\delta\mathbf{x}(t)\delta x(t) + 2\bar{\mathbf{v}}\delta x^2(t)]\,\mathrm{erfc}\frac{t\bar{v} - \delta x(t)}{t^{1/2}} \\ & \left. - \frac{\sqrt{\pi}}{4\delta x^3(t)} e^{2\bar{v}\delta x(t)}[\delta\mathbf{x}(t) - 2\bar{v}\delta x(t)\delta\mathbf{x}(t) + 2\bar{\mathbf{v}}\delta x^2(t)]\,\mathrm{erfc}\frac{t\bar{v} + \delta x(t)}{t^{1/2}}\right\}. \end{aligned} \tag{B9}$$

2. Early-time asymptotic expansion

Consider now the early-time limit $t \searrow 0$ of the particle velocity $\mathbf{v}(t)$ in the same scenario as described above (B1), with the force $\mathbf{f}(t)$ assumed to be smooth for $t > 0$, with a finite limit $\mathbf{f}(t) \to \mathbf{f}_+$ as $t \searrow 0$ that may differ from the constant force value $\mathbf{f}_-$ corresponding to the steady state $\mathbf{v}(t) = \bar{\mathbf{v}}$ for $t < 0$ [cf. Eq. (B1)].

We claim that the particle velocity possesses an expansion of the form

$$\mathbf{v}(t) = \bar{\mathbf{v}} + t^{1/2}\mathbf{v}_1 + \mathcal{O}(t) \quad \text{as } t \searrow 0, \tag{B10}$$

where the fractional powers are suggested by the form of the history operator (5.2) and we have assumed that the velocity is continuous at $t = 0$. It can be shown that without the latter assumption the history operator is asymptotically large as $t \searrow 0$, with no other comparable term in the amplitude equation (5.1) to balance it.

Consider now the history operator $\mathbf{H}[\mathbf{v}](t)$ as $t \searrow 0$. Carefully expanding the closed-form expression for the tail contribution (B9) gives

$$\mathbf{H}^{-}[\mathbf{v}(\tau)]^{t}_{\tau=0}(t;\bar{\mathbf{v}}) = \frac{28}{9\sqrt{\pi}}\mathbf{v}_1 + \mathcal{O}(t^{1/2}) \quad \text{as } t \searrow 0, \tag{B11}$$

where we have used Eqs. (B7) and (B10) to obtain $\delta\mathbf{x} = 2t^{3/2}\mathbf{v}_1/3 + \mathcal{O}(t^2)$ in the same limit. Consider next the contribution (B4) from positive past times. Upon making the change of variables $p = t - \tau$, we have

$$\mathbf{H}^{+}[\mathbf{v}(\tau)]^{t}_{\tau=0}(t;\bar{\mathbf{v}}) = \frac{2}{\sqrt{\pi}}\int_0^t \frac{dp}{p^{5/2}}\left\{p\mathbf{v}(t)e^{-pv^2(t)} - \mathbf{x}'(t-p,t)e^{-\frac{|\mathbf{x}'(t-p,t)|^2}{p}}\right\}. \tag{B12}$$

Noting that [cf. Eq. (4.9)]

$$\mathbf{x}'(t-p,t) = \bar{\mathbf{v}}p + \tfrac{2}{3}\mathbf{v}_1[t^{3/2} - (t-p)^{3/2}] + \mathcal{O}(t^2) \quad \text{as } t \searrow 0, \tag{B13}$$

a straightforward expansion of Eq. (B12) gives

$$\mathbf{H}^{+}[\mathbf{v}(\tau)]^{t}_{\tau=0}(t;\bar{\mathbf{v}}) = \frac{4(3\pi - 7)}{9\sqrt{\pi}}\mathbf{v}_1 + \mathcal{O}(t^{1/2}) \quad \text{as } t \searrow 0. \tag{B14}$$

Combining the contributions (B11) and (B14) then gives

$$\mathbf{H}[\mathbf{v}] = \frac{4\sqrt{\pi}}{3}\mathbf{v}_1 + \mathcal{O}(t^{1/2}) \quad \text{as } t \searrow 0. \tag{B15}$$

Using Eqs. (B10) and (B15) to expand the amplitude equation (5.1), we find

$$\mathbf{v}_1 = \frac{3}{16\sqrt{\pi}}[(\chi - 16\bar{v})\bar{\mathbf{v}} + 2\mathbf{f}_+]. \tag{B16}$$

Clearly, $\mathbf{v}_1$ vanishes if and only if the force is continuous at $t = 0$, that is if $\mathbf{f}_+ = \mathbf{f}_-$.

APPENDIX C: NUMERICAL REGULARIZATION

In our numerical scheme, the contribution (B4) of positive past times is evaluated by the trapezoidal rule. The integrable $1/(t-\tau)^{1/2}$ singularity of the integrand [cf. Eq. (C3)] induces a $\mathcal{O}(\Delta t^{1/2})$ discretization error, where Δt is the time step. To improve on this, we note that for $t > 0$ we have

$$\mathbf{x}'(\tau, t) = (t-\tau)\mathbf{v}(t) - \tfrac{1}{2}(t-\tau)^2\mathbf{a}(t) + \mathcal{O}[(t-\tau)^3] \quad \text{as } \tau \nearrow t, \tag{C1}$$

where $\mathbf{a}(t) = d\mathbf{v}(t)/dt$ is the acceleration. It follows that in the same limit

$$-\mathbf{x}'(\tau, t)e^{-\frac{|\mathbf{x}'(\tau,t)|^2}{t-\tau}} = e^{-(t-\tau)v^2(t)}\left\{-(t-\tau)\mathbf{v}(t) + \tfrac{1}{2}(t-\tau)^2\mathbf{a}(t)\right\} + \mathcal{O}[(t-\tau)^3], \tag{C2}$$

where for later convenience we do not expand the exponent on the right-hand side. Thus, the integrand in Eq. (B4) possesses the expansion

$$\frac{\mathbf{a}(t)}{(t-\tau)^{1/2}}e^{-(t-\tau)v^2(t)} + \mathcal{O}[(t-\tau)^{1/2}] \quad \text{as } \tau \nearrow t \tag{C3}$$

and so Eq. (B4) can be regularized by subtracting and adding the integral

$$\frac{\mathbf{a}(t)}{\sqrt{\pi}}\int_0^t \frac{d\tau}{(t-\tau)^{1/2}}e^{-(t-\tau)v^2(t)} = \mathbf{a}(t)\frac{\operatorname{erf}[t^{1/2}v^{1/2}(t)]}{v^{1/2}(t)}. \tag{C4}$$

This reduces the order of the discretization error to $\Delta t^{3/2}$ with the small penalty of having to estimate the acceleration $\mathbf{a}(t)$ as part of the numerical scheme.

APPENDIX D: LINEAR IMPULSE RESPONSE

The linear stability analysis in Sec. V C assumes an exponential time dependence $\delta\mathbf{v} = \mathbf{A}e^{\sigma t}$, and results in equations (5.9) and (5.10) for the growth rate σ which can be written in the form $F(\sigma) = 0$, where

$$F(\sigma) = -\chi + \frac{32\sigma^{1/2}}{3} \quad \text{and} \quad -\chi + \frac{32}{3}\left[\frac{(\bar{v}^2+\sigma)^{3/2} - \bar{v}^3}{\sigma} + 3\delta_\parallel\bar{v}^2\frac{(\bar{v}^2+\sigma)^{1/2} - \bar{v}}{\sigma}\right], \tag{D1}$$

respectively, for the static base state with $\bar{\mathbf{v}} = \mathbf{0}$ and for the steady rectilinear-motion base state with $\bar{\mathbf{v}} \neq \mathbf{0}$ (and $\delta_\parallel = 1$ for $\mathbf{A} \parallel \bar{\mathbf{v}}$ or $\delta_\parallel = 0$ for $\mathbf{A} \perp \bar{\mathbf{v}}$). These equations are only valid for $\operatorname{Re}\sigma \geqslant -\bar{v}^2$, as the linearized history integral (4.22) diverges otherwise. Here, we seek to calculate the decay rates of the perturbations when there is no such solution σ.

We do this by considering the linear response to a force impulse of amplitude $\mathbf{B}$, i.e., the solution $\delta\mathbf{v}(t)$ to

$$\{\chi - 16\bar{v}(\mathsf{I} + \hat{\bar{\mathbf{v}}}\hat{\bar{\mathbf{v}}})\} \cdot \delta\mathbf{v} - 4\,\delta\mathbf{H}[\delta\mathbf{v}; \bar{\mathbf{v}}] = 2\mathbf{B}\delta(t) \tag{D2}$$

that satisfies $\delta\mathbf{v}(t) = 0$ for $t < 0$, where $\delta(t)$ is the Dirac δ function. Using a Laplace transform,

$$\mathcal{L}\{\delta\mathbf{v}\}(s) = \int_{0^-}^{\infty} dt\, \delta\mathbf{v}(t) e^{st}, \tag{D3}$$

and evaluating Eq. (4.23) or Eq. (4.25), we obtain the result

$$F(s)\mathcal{L}\{\delta\mathbf{v}\} = 2\mathbf{B}, \tag{D4}$$

where the function $F(s)$ is given by Eq. (D1). The solution is then given by the Laplace inversion integral

$$\delta\mathbf{v}(t) = \frac{\mathbf{B}}{\pi i} \int_{c-i\infty}^{c+i\infty} ds\, \frac{e^{st}}{F(s)}, \tag{D5}$$

where the contour passes to the right of any singularities of the integrand. We determine the late-time behavior of this integral using the method of steepest descent. The calculation of $F(s)$ requires $\mathrm{Re}\, s \geqslant -\bar{v}^2$ for the history integral to converge, so we extend the results (D1) analytically, placing the branch cut for the square roots on the real axis where $s < -\bar{v}^2$. A suitable steepest-descent contour then runs just below the branch cut from $-\infty$ to the branch point $-\bar{v}^2$, anticlockwise around the branch point, and then just above the branch cut back to $-\infty$.

We first consider the static base state, $\bar{\mathbf{v}} = \mathbf{0}$. For $\chi < 0$, the equation $F(\sigma) = 0$ has no solutions, so we can deform onto the steepest-descent contour without crossing any singularities of the integrand. We then use the parametrization $s = -x$ to obtain

$$\delta\mathbf{v} = \frac{\mathbf{B}}{\pi i} \int_0^{\infty} dx \left[\frac{-1}{\chi + i\frac{32}{3}x^{1/2}} + \frac{1}{\chi - i\frac{32}{3}x^{1/2}} \right] e^{-xt} = \frac{64\mathbf{B}}{3\pi} \int_0^{\infty} dx\, \frac{x^{1/2}\, e^{-xt}}{\chi^2 + \frac{1024}{9}x}, \tag{D6}$$

from which Watson's lemma yields the leading-order behavior

$$\delta\mathbf{v} \sim \frac{32\mathbf{B}}{3\sqrt{\pi}\chi^2} t^{-3/2} \quad \text{as } t \to \infty. \tag{D7}$$

For $\chi = 0$, the same contour yields an exact result

$$\delta\mathbf{v} = \frac{3\mathbf{B}}{16\pi} \int_0^{\infty} dx\, \frac{e^{-xt}}{x^{1/2}} = \frac{3\mathbf{B}}{16\sqrt{\pi}} t^{-1/2}. \tag{D8}$$

For $\chi > 0$, the contribution from the contour is again given by Eq. (D6), but the contour deformation crosses a pole, located at the solution $s = \sigma$ of $F(\sigma) = 0$, and picks up a residue contribution (that is exponentially dominant over the contour contribution), so that

$$\delta\mathbf{v} \sim \frac{2\mathbf{B}e^{\sigma t}}{F'(\sigma)} = \frac{3\mathbf{B}\sigma^{1/2}e^{\sigma t}}{8}, \tag{D9}$$

which we recognize as the exponential behavior predicted in Sec. V C, but with amplitude determined by the impulse amplitude.

For steady rectilinear motion $\bar{\mathbf{v}} \neq \mathbf{0}$, the calculation proceeds in the same way. Using the parametrization $s = -\bar{v}^2(1 + x)$, we express the steepest-descent integral as

$$\frac{64\mathbf{B}\bar{v}e^{-\bar{v}^2 t}}{3\pi} \int_0^{\infty} dx\, \frac{(1+x)(x - 3\delta_{\parallel})x^{1/2}}{\left[(1+x)\chi/\bar{v} - \frac{32}{3}(1 + 3\delta_{\parallel})\right]^2 + \frac{1024}{9}x(3\delta_{\parallel} - x)^2} e^{-x\bar{v}^2 t}. \tag{D10}$$

Thus, when $F(\sigma) = 0$ has no solutions with $\mathrm{Re}\,\sigma \geqslant -\bar{v}^2$, Watson's lemma yields the leading-order results, as $t \to \infty$,

$$\delta\mathbf{v} \sim -\frac{32\mathbf{B}}{\sqrt{\pi}\left(\chi - \frac{128}{3}\bar{v}\right)^2} e^{-\bar{v}^2 t} t^{-3/2} \quad \text{or} \quad \delta\mathbf{v} \sim \frac{16\mathbf{B}\bar{v}^{-2}}{\sqrt{\pi}\left(\chi - \frac{32}{3}\bar{v}\right)^2} e^{-\bar{v}^2 t} t^{-5/2}, \tag{D11}$$

depending on whether the perturbation is longitudinal or transverse, respectively. If, however, there are such solutions σ, then the associated residue contributions are dominant, yielding exponential solutions (except that for $\chi = 32\bar{v}$ the solution $\sigma = 0$ is a double root, leading to a perturbation of the form $\delta\mathbf{v} \sim at + b$).

We conclude that, for all three cases, when the growth-rate equation $F(\sigma) = 0$ has a solution with $\mathrm{Re}\,\sigma > -\bar{v}^2$, then there are perturbations with exponential time dependence $e^{\sigma t}$. If there are no such solutions, then the perturbations decay like $e^{-\bar{v}^2 t}$ times a power of t, and hence the base state is stable, as was asserted in Sec. V C.

[1] S. Michelin, E. Lauga, and D. Bartolo, Spontaneous autophoretic motion of isotropic particles, Phys. Fluids **25**, 061701 (2013).

[2] R. Golestanian, T. B. Liverpool, and A. Ajdari, Propulsion of a Molecular Machine by Asymmetric Distribution of Reaction Products, Phys. Rev. Lett. **94**, 220801 (2005).

[3] R. Golestanian, T. B. Liverpool, and A. Ajdari, Designing phoretic micro-and nano-swimmers, New J. Phys. **9**, 126 (2007).

[4] S. Michelin, Self-propulsion of chemically active droplets, Ann. Rev. Fluid Mech. **55**, 77 (2023).

[5] O. Schnitzer, Weakly nonlinear dynamics of a chemically active particle near the threshold for spontaneous motion. I. Adjoint method, Phys. Rev. Fluids **8**, 034201 (2023).

[6] A. Y. Rednikov, Y. S. Ryazantsev, and M. G. Velarde, Drop motion with surfactant transfer in a homogeneous surrounding, Phys. Fluids **6**, 451 (1994).

[7] A. Y. Rednikov, Y. S. Ryazantsev, and G. Velárde, M, Drop motion with surfactant transfer in an inhomogeneous medium, Int. J. Heat Mass Transf. **37**, 361 (1994).

[8] M. Morozov and S. Michelin, Nonlinear dynamics of a chemically-active drop: From steady to chaotic self-propulsion, J. Chem. Phys. **150**, 044110 (2019).

[9] M. Morozov and S. Michelin, Self-propulsion near the onset of Marangoni instability of deformable active droplets, J. Fluid Mech. **860**, 711 (2019).

[10] S. Saha, E. Yariv, and O. Schnitzer, Isotropically active colloids under uniform force fields: From forced to spontaneous motion, J. Fluid Mech. A **916**, 47 (2021).

[11] A. Farutin and C. Misbah, Singular bifurcations: a regularization theory, arXiv:2112.12094.

[12] E. Yariv and U. Kaynan, Phoretic drag reduction of chemically active homogeneous spheres under force fields and shear flows, Phys. Rev. Fluids **2**, 012201(R) (2017).

[13] R. Kailasham and A. S. Khair, Dynamics of forced and unforced autophoretic particles, J. Fluid Mech. **948**, A41 (2022).

[14] A. C. Castonguay, R. Kailasham, C. M. Wentworth, C. H. Meredith, A. S. Khair, and L. D. Zarzar, Gravitational settling of active droplets, Phys. Rev. E **107**, 024608 (2023).

[15] H. A. Stone and A. D. T. Samuel, Propulsion of Microorganisms by Surface Distortions, Phys. Rev. Lett. **77**, 4102 (1996).

[16] A. Acrivos and T. D. Taylor, Heat and mass transfer from single spheres in Stokes flow, Phys. Fluids **5**, 387 (1962).

[17] Z.-G. Feng and E. E. Michaelides, Unsteady heat transfer from a sphere at small Peclet numbers, J. Fluids Eng. **118**, 96 (1996).

[18] C Pozrikidis, Unsteady heat or mass transport from a suspended particle at low Peclet numbers, J. Fluid Mech. **334**, 111 (1997).

[19] M. Abramowitz and I. A. Stegun, *Handbook of Mathematical Functions*, 3rd ed. (Dover, New York, NY, 1965).

[20] A. Y. Rednikov, V. N. Kurdyumov, Y. S. Ryazantsev, and M. G. Velarde, The role of time-varying gravity on the motion of a drop induced by Marangoni instability, Phys. Fluids **7**, 2670 (1995).

[21] K. Lippera, M. Morozov, M. Benzaquen, and S. Michelin, Collisions and rebounds of chemically active droplets, J. Fluid Mech. **886**, A17 (2020).

[22] A. Farutin, M. S. Rizvi, W. F. Hu, T. S. Lin, S. Rafai, and C. Misbah, A reduced model for a phoretic swimmer, J. Fluid Mech. **952**, A6 (2022).
[23] K. Lippera, M. Benzaquen, and S. Michelin, Alignment and scattering of colliding active droplets, Soft Matter **17**, 365 (2021).
[24] Y. Chen, K. L. Chong, L. Liu, R. Verzicco, and D. Lohse, Instabilities driven by diffusiophoretic flow on catalytic surfaces, J. Fluid Mech. **919**, A10 (2021).
[25] N. Desai and S. Michelin, Instability and self-propulsion of active droplets along a wall, Phys. Rev. Fluids **6**, 114103 (2021).
[26] F. Picella and S. Michelin, Confined self-propulsion of an isotropic active colloid, J. Fluid Mech. **933**, A27 (2022).
[27] N. Desai and S. Michelin, Steady state propulsion of isotropic active colloids along a wall, Phys. Rev. Fluids **7**, 100501 (2022).
[28] B. V. Hokmabad, J. Agudo-Canalejo, S. Saha, R. Golestanian, and C. C. Maass, Chemotactic self-caging in active emulsions, Proc. Natl. Acad. Sci. USA **119**, e2122269119 (2022).